THE SPIRAL GROWTH OF CRYSTALS

A. A. CHERNOV

CONTENTS

THE classical ideas regarding the mechanism involved in the formation of the crystalline phase of matter were formulated by Gibbs,[1] and were developed by Volmer,[2] Kossel,[3] Stranski,[4,5] Kaischew,[6-9] Becker and Döring,[10] and others. According to the classical theory, the ideal " close-packed" (or dense-packed) face of a growing crystal advances at a rate that is proportional to the frequency with which the nuclei of new atomic (or molecular) layers are created on the given face. (These are the so-called two-dimensional nuclei.) The probability of nucleation, and therefore the growth rate of a face, is negligibly small until supersaturation reaches the order of a few tens

percent. The advance of the edges of uncompleted layers, i.e., steps (Fig. 1), is then rapid, and does not furnish an additional factor limiting the crystallization rate. The conclusions arrived at in the classical theory were confirmed in specific experiments.[2,11]

In an enormous number of instances, however, crystals grow even at less than 1% supersaturation, just as though the problem of nucleation did not exist for them. Morphological studies of the surfaces of these crystals have revealed a large number of steps varying in height from one lattice parameter to many hundreds or thousands of lattice parameters. The sources of these steps are the contacts between crys-
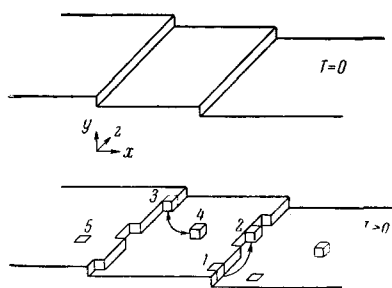
FIG. 1. Steps on the surface of a crystal at T = 0 and T > 0. Particles denoted by cubes are 1 — edge components of an incomplete layer (i.e., step), 2 — adsorbed on a step, 3 — faces of kinks, 4 — adsorbed on the surface, 5 — vacancies in the surface atomic layer. The arrow between 3 and 4 symbolizes exchange between kinks and an adsorbed layer, and that between 1 and 2 symbolizes the creation of kinks by fluctuations.

tals and holders, intergranular boundaries, foreign macroscopic particles, and the surface points at which screw dislocations emerge (Ch. II, III). It was first shown by Frank[12] that a dislocation intersecting a crystal surface produces a step that does not disappear during the growth process. Nucleation of a new surface is unnecessary when a screw dislocation is present.

When the rate of growth is not limited by slow step formation, the entire kinetics is determined by the motion of steps already existing, and by their shapes, relative positions, heights, interactions with each other and with dislocations and impurities etc. The present article discusses the layer growth of crystals. Chapter I investigates the structure of a crystal surface in equilibrium with the surrounding medium, considering several general questions with regard to crystalline surface energy, as well as the creation and stability of macroscopic steps on the surfaces of crystals.

The kinetics of layer growth from the gaseous phase, solutions, and melts is discussed in Ch. II and III, essentially on the basis of dislocations as sources of steps. Chapter IV deals with impurity capture and with the effect of impurities on the growth rate.

Certain basic ideas regarding the mechanisms of selective etching are explained in Ch. V.

Chapter VI discusses the statistical approach to the description of collective effects in the motion of different steps on a crystal surface, and specifically the kinetic equation for steps.

The present review gives no account of the results obtained in the aforementioned classical publications on the theory of crystal growth. The reader can find these, for example, in the books by Volmer[2] and Buckley,[86] and more concisely in the books by Shubnikov[137-139] and by Obreimov.[140]

Among the comprehensive publications on the mod-

ern dislocation theory of spiral growth, to the development of which the present review is devoted, one must mention first of all the original paper by Burton, Cabrera, and Frank,[14] the authors of the theory, and the books by Varma,[44] Amelinckx and Dekeyser,[37] and Friedel.[144]

The general aspects of the kinetics of phase transitions and, specifically, of crystal growth, are discussed in a review article by Turnbull.[76]

The proceedings of conferences on crystal growth are also of interest.[141-143]

I. CRYSTAL SURFACES IN EQUILIBRIUM WITH THE SURROUNDING MEDIUM. THE SURFACE ENERGY OF CRYSTALS

As already mentioned in the introduction, the kinetics of crystal growth depends on surface structure, including both the microscopic atomic (or molecular) structure and macroscopic steps.

The present chapter deals with the structure of crystal surfaces in equilibrium with the surrounding medium. The most important feature of microscopic surface structure is the existence of kinks — reentrant trihedral corners in elementary (monolayer) steps, which are one interatomic spacing in height (configuration 3, Fig. 1). Large numbers of kinks are created by fluctuations, and play an extremely important part in crystal growth, since they provide the sites at which new atoms or molecules are added to crystals. The formation of kinks is discussed in Sec. 1.

A crystal surface composed of elementary steps does not generally possess minimum surface energy; its shape will therefore change. It will be shown in Sec. 4 that the conditions for minimum surface energy require the merging of elementary steps and the creation of macroscopic steps whenever the equilibrium shape of a bounded closed crystal (according to Wulff) possesses edges (i.e., practically always at low temperatures). This points to a general condition where the surface energy favors the stability of surface form while the form is nevertheless, unstable.

1. Kinks in Elementary Steps[13,14]

Steps are found on a crystalline surface that is slightly inclined from the orientation corresponding to any close-packed face [such as the (1, 10, 0) surface of a cubic crystal in Fig. 1]. The steps can have any height beginning with one interatomic spacing (an elementary step). Let there be a (0, 1) step in the close-packed (0, 1, 0) plane (Fig. 1). At absolute zero (T = 0) the front of the step will be atomically smooth. When T > 0, fluctuations lead to the appearance of kinks, i.e., trihedral corners in the step (configuration 3, Fig. 1).

For a step making the small angle θ with the z

axis, the mean distance between kinks is

$$\lambda_\theta = \left\{ 1 - \frac{1}{2}\left(\frac{\lambda_0}{a}\right)^2 \theta^2 \right\} ,$$ (1.1)

where

$$\lambda_c = \frac{a}{2}\left\{ e^{\frac{w_1}{kT}} + 2 \right\}$$ (1.2)

is the separation of kinks for a close-packed step parallel to the z axis (a is the interatomic spacing), and w_1 is the formation energy of a single kink.

In the passage of a single atom (or molecule) from a position in a step (position 1, Fig. 1) to an adsorbed position (position 2) four kinks are formed. In the case of a (11) step on a (111) face of a face-centered cubic lattice this transition breaks two bonds between nearest neighbors, i.e., one-third of the energy of crystallization W is thus expended. Therefore $w_1 = \frac{1}{12}W$. When vapor surrounds the crystal, W is the energy of sublimation. Taking $W/kT = 24$, we obtain from (1.2):

$$\lambda_0 \sim \frac{1}{2} a \exp\left(\frac{w_1}{kT}\right) \sim 4a.$$

For a (10) step on a (100) face of a simple cubic crystal, assuming interactions only between nearest neighbors, $w_1 \sim \frac{1}{6}W$, and the separation of dislocations must be $\sim 30a$. This distance is reduced when next nearest neighbors are taken into account.

The presence of kinks in a step changes the free energy per unit length of the step front, as well as its anisotropy. This is shown schematically by the dashed lines in Fig. 2a.
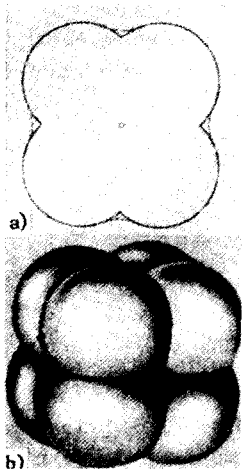

FIG. 2. Polar diagram of surface energy a) in the two-dimensional case (solid curve at T = 0, dashed curve at T > 0); b) in the three-dimensional case.

2. Crystal Surface Energy. Herring's Formula

We turn now to the phenomenological description of macroscopic surface structure, and shall begin with certain general properties of the surface energy.

The free energy of a unit surface element will be denoted by $\alpha(n)$, where n is the normal to this element and indicates its orientation. For values of n representing close-packed faces, $\alpha(n)$ has a sharp minimum, such that the derivatives $\frac{\partial \alpha}{\partial \varphi}$ and/or $\frac{\partial \alpha}{\partial \theta}$ become discontinuous here (φ and θ being spherical coordinate angles), i.e., the surface $\alpha(\varphi, \theta)$ exhibits corner points and lines[15-17] (Fig. 2b). Fluctuation smearing of the sharp minima of surface specific energy, similar to the spreading of minima in the case of the linear specific energy of a step (Fig. 2a), can only occur for certain faces near the melting point (reference 14) and does not usually take place. Since the edges and vertices of a macroscopic crystal are equivalent to steps with regard to the possibility of fluctuations, these edges and vertices must be smeared off at $T > 0$.

The chemical potential μ_m of a medium in equilibrium with a crystal possessing a smooth surface (i.e., without macroscopic corners and edges) is given by

$$\mu_m = \mu_{C0} + \Omega k_1\left(\alpha + \frac{\partial^2 \alpha}{\partial \varphi_1^2} \right) + \Omega k_2\left(\alpha + \frac{\partial^2 \alpha}{\partial \varphi_2^2} \right),$$ (2.1)

where μ_{C_0} is the chemical potential of an infinite crystal with a plane surface, Ω is its atomic (or molecular) specific volume, k_1 and k_2 are the curvatures of the crystal surface in the planes of its principal sections through the considered point, and φ_1 and φ_2 are angles measured in these planes. Equation (2.1) was derived by Herring,[18,19] and extends Thomson's familiar formula for liquids.

We shall now determine the relationship[20] between (2.1) and the familiar problem of the equilibrium shape $z(x, y)$ of a bounded crystal with constant volume (see references 17 and 21, for examples):

$$\iint \alpha(n)\, ds = \min, \quad \iint z(x, y)\, dx\, dy = \text{const.}$$ (2.2)

The solution is the envelope of the family of planes

$$(n, r) = \alpha(n)\, \Lambda^{-1},$$ (2.3)

where r is the radius vector of a point on each plane, and n, as previously, is the normal to the crystal surface. The constant Λ is the Lagrangian multiplier of the variational problem (2.2) that arises from the condition of constant volume.

Equation (2.3) expresses the familiar Wulff theorem to the effect that the minimum surface energy corresponds to a surface which is the envelope of planes perpendicular to the radius vectors through each point of the polar diagram of crystalline surface energy. In other words, the distances between the center of a crystal with equilibrium shape and its faces are proportional to the surface specific energies of these faces.

We first ascertain that the product $\Omega\Lambda$ has the physical meaning of a supplementary chemical poten-

tial associated with the surface energy. Indeed, we require constancy of the chemical potential μ_m of the medium above the entire surface of the crystal, i.e., of $\mu_m = \mu_{C_0} + \Omega \tilde{\Lambda}$, or

$$k_1(\alpha + \alpha''_{\varphi_1 \varphi_1}) + k_2(\alpha + \alpha''_{\varphi_2 \varphi_2}) = \tilde{\Lambda}, \qquad (2.4)$$

where $\tilde{\Lambda}$ is a constant. Equation (2.4) is the differential equation of the surface shape which satisfies the condition of constant μ_m. On the other hand, from the method of deriving (2.1), Eq. (2.4) is the Lagrangian equation of the variational problem (2.2) with the Lagrangian constant Λ. Therefore $\tilde{\Lambda} = \Lambda$, and $\Omega \Lambda$ is the departure of the chemical potential of a medium in equilibrium with the given crystal, from the value required for equilibrium between the medium and an infinite crystal (for which $\Lambda = 0$). The constant Λ and the left-hand side of (2.4) have the dimensions of pressure.

As shown at the beginning of this section, the anisotropy of $\alpha(n)$ is such that for surface orientations corresponding to close-packed faces, the first derivatives α'_{φ_1} and α'_{φ_2} are discontinuous, i.e., the second derivatives in (2.4) are infinite. Therefore, on close-packed faces, the supplementary chemical potential of the crystal will be finite only when the curvatures k_1 and k_2 vanish (the corresponding surfaces become planes). This dictates the physical requirement of plane faces on crystals of equilibrium shape.

In the case of nonequilibrium shapes the left-hand side of (2.4) is not constant and the chemical potential of the medium varies over different portions of the crystalline surface. When, for example, the medium is a solution, its concentration varies on the surface. As a result, diffusion begins, leading to the dissolution of some parts and the growth of other parts of the crystal. This process terminates only when the crystal assumes its equilibrium shape, with the concentration of the solution (more accurately, the chemical potential) becoming uniform over the entire surface.

3. Corner Points in the Profiles of Crystal Surfaces[22]

The solution of (2.2) is the envelope of the family of planes (2.3), and, because of the anisotropy of α, generally contains self-intersecting and self-reversing lines (Fig. 3). Since such configurations are meaningless on a real physical surface, we must investigate specifically the possibility of the existence of corner lines on the crystal surface, as well as their stability.

For the sake of simplicity, we shall investigate the two-dimensional case of the contour $y(x)$ with line specific free energy $\alpha(p)$ where $p \equiv \dfrac{dy}{dx}$. The contour can be treated as the section of the (x, y) plane by a cylindrical surface that is infinite in the z direction. We shall therefore speak of the surface energy of the contour (rather than of its line energy), meaning the surface energy per unit length in the z direction.
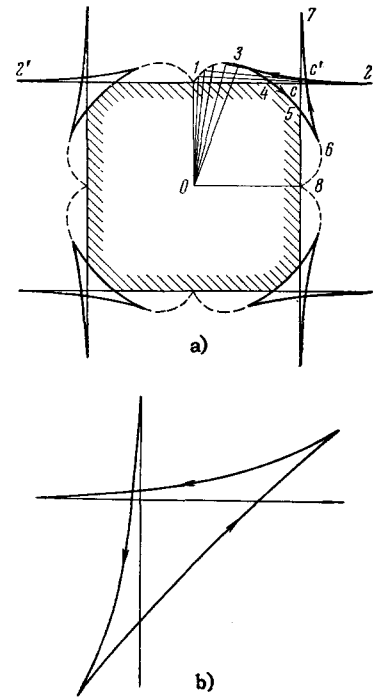

FIG. 3. a) Polar diagram of surface energy (dashed curve); envelope plotted from Wulff's theorem (solid curve). The shaded interior of the envelope depicts the equilibrium shape of the crystal. b) The upper left-hand corner of the Wulff envelope for surface-energy anisotropy differing somewhat from that in a).

We now drop the assumption (made in Sec. 2) of smoothness of $y(x)$, and permit the existence of corner points on $y(x)$. Above the portions of a two-dimensional crystal that are bounded by a smooth contour, the chemical potential of the medium is determined, as previously, from Herring's formula (2.1) (here for the two-dimensional case). We now determine the supplementary chemical potential μ_C of the crystal associated with the corner point (x_c, y_c). Transferring δN particles to the crystal in the vicinity of a corner point (Fig. 4) and attributing to δN the required change $\delta \int \alpha \, ds$ of contour energy, we obtain

$$\frac{\delta \int \alpha \, ds}{\delta N} = [F'_p] \frac{\delta x}{\delta N} + [pF'_p - F] \frac{\delta y_c}{\delta N}, \qquad (3.1)$$

where $(\delta x_c, \delta y_c)$ is the displacement of the corner point in the variational process, and

$$F(p) \equiv \alpha(p) \sqrt{1 + p^2},$$

$$F'_p \equiv \frac{\partial F}{\partial p}, \quad [A] \equiv A\,|_{p=p(x_c+0)} - A\,|_{p=p(x_c-0)}.$$

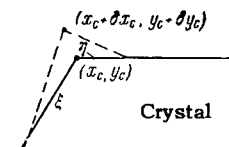The supplementary term is obtained for $\delta N \to 0$. Figure 4 shows that

FIG. 4

$$\delta N \sim \frac{1}{\Omega}(\xi + \eta)\sqrt{(\delta x_c)^2 + (\delta y_c)^2}$$

and, consequently, as δx_c, δy_c, ξ and η approach zero the right-hand side of (3.1) will increase without limit in all cases except when

$$F'_p|_{p=p_-} = F'_p|_{p=p_+}, \qquad pF'_p - F|_{p=p_-} = pF'_p - F|_{p=p_+}, \qquad (3.2)$$

where $p_- = p(x_c - 0)$ is the tangent of the slope of the contour to the left, and $p_+ = p(x_c + 0)$ is that to the right of the corner point (x_c, y_c). In other words, the supplementary chemical potential of the crystal for a contour $y(x)$ possessing a corner point is infinite whenever the orientation of the surface profile to the left and to the right of that corner does not satisfy (3.2). Whenever (3.2) is fulfilled the additional term vanishes, and the chemical potential of the medium above the surface of the crystal is given by Herring's formula, using the curvature of the smooth parts of the contour.

Thus when the system (3.2) in the two unknowns p_+ and p_- has one or more nontrivial solutions* (such that $p_+ \neq p_-$), the given surface profile can exhibit corner points, where the contour direction is discontinuous while the slope on both sides of each point is determined by pairs of roots of (3.2).

Since the supplementary chemical potential term (3.1) is either zero or infinite [when (3.2) is not satisfied], the configuration determined by (3.2) will exist not only when the crystal and surrounding medium are in equilibrium, but also for small departures from equilibrium, i.e., in crystal growth or dissolution. Therefore the contour shape determined by (3.2) is extremely stable† with respect to small departures from equilibrium. With large departures, considerable probability exists for disruption of the surface shape by a finite rather than infinitely small amount (δN is finite and does not approach zero), i.e., the nucleation process, which requires surmounting of the potential barrier and is thus only possible under considerable supersaturation.

When (3.2) has no nontrivial solution in the form of a pair of actually different roots, corner points will not exist on the surface profile. The surface will then be macroscopically smooth (rounded, without vertices).

Equation (3.2) could be derived formally as the equations for contour slopes at self-intersection points of the curve for $x(p, \Lambda)$, $y(p, \Lambda)$, where $p = dy/dx$ is a parameter:

$$\Lambda x = F'_p(p) + \text{const}, \qquad \Lambda y = pF'_p(p) - F(p) + \text{const}. \qquad (3.3)$$

This curve results from integrating the Lagrangian equation of the variational problem for the equilibrium shape of a smooth curve. This shows the equivalence of the self-intersection points and the corner points determined from (3.2).

---

*If p_+ and p_- are roots of (3.2), p_+^{-1} and p_-^{-1} will also be roots.

†The minimization of the energy [Eq. (4.1)] must also be satisfied.

The conditions (3.2) have the simple geometrical meaning that at the points p_+ and p_- the tangents to the curve $F(p)$ must coincide (Fig. 5a).
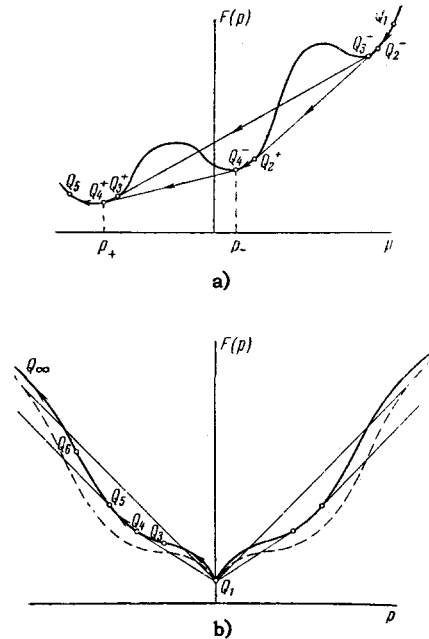

FIG. 5. a) Schematic representation of the function $F(p) = \alpha(p)\sqrt{1 + p^2}$. Values of p, such as p_+ and p_-, where double tangents to $F(p)$ are possible ($Q_2^- Q_4^+$, $Q_3^- Q_3^+$, $Q_4^- Q_4^+$) determine the slope of the crystalline surface to the right and left of a corner point. b) Plots of the functions $F(p)$ corresponding to the Wulff envelopes in Fig. 3 (the solid curve for Fig. 3a and the dashed curve for Fig. 3b).

4. Surface Stability Conditions

All solutions obtained so far satisfy the condition for constancy of the chemical potential over the entire crystalline surface, and are extremal since they ensure vanishing of the first variation $\delta \int \alpha\, ds$ of the surface energy. However, minimization also requires a positive value for the second variation of $\int \alpha\, ds$, i.e., on smooth regions:

$$\delta^2 \int F(p)\, dx = \frac{1}{2}\int \frac{\partial^2 F}{\partial p^2}(\delta p)^2\, dx > 0, \qquad (4.1)$$

whence

$$\frac{\partial^2 F}{\partial p^2} > 0 \quad \text{or} \quad \alpha + \alpha''_{\varphi\varphi} > 0, \qquad (4.1a)$$

where $\varphi = \tan^{-1} p$. Consequently, the surface energy permits the stability only of regions whose profile does not contain orientations φ leading to $\alpha + \alpha'' < 0$.

The condition (4.1a) denotes positive curvature of $F(p)$. Thus thermodynamically stable macroscopically smooth surface regions must have slopes corresponding to segments of $F(p)$ that are concave upwards. Stability disappears at inflection points, where

$$\frac{\partial^2 F}{\partial p^2} = 0.$$

Not all the corner points satisfying (3.2) are associ-

ated with an absolute minimum of the surface energy, and therefore not all of them can exist on a real surface under conditions of equilibrium. Equation (4.1a) for corner points is equivalent to the statement that the only stable corner points on a surface profile are those for which the tangent to $F(p)$ that determines the profile slope discontinuity at a given corner point occupies the lowest position. For example, in Fig. 5a, of all possible corner points corresponding to the tangents $Q_2^- Q_2^+$, $Q_4^- Q_4^+$ and $Q_3^- Q_3^+$, only those corresponding to $Q_2^- Q_2^+$ and $Q_4^- Q_4^+$ will be stable on a real surface. The simple proof for this will not be given here.

To sum up, we shall establish the correspondence between motion along $F(p)$ and motion along the Wulff envelope for $\Lambda^{-1}F(p)$. $F(p)$ is depicted qualitatively in Fig. 5b (solid curve), and the Wulff envelope in Fig. 3a. The orientation $p = 0$ [the point Q_1 on $F(p)$] corresponds to a close-packed face; here $\alpha(p)$ has a sharp minimum, where $\dfrac{\partial^2 F}{\partial p^2} = \infty$. On the equilibrium shape the point Q_1 corresponds to the rectilinear segment (the close-packed face) connecting the points 2' and 2. The length of segment 2'2 (but not of the equilibrium face!) is $\Lambda^{-1}\left[\dfrac{\partial \alpha}{\partial \varphi}\right]$, where $\left[\dfrac{\partial \alpha}{\partial \varphi}\right]$ is the discontinuity of the derivative $\dfrac{\partial \alpha}{\partial \varphi}$ for $\varphi = 0$. The segment $Q_1 Q_3$ of $F(p)$ corresponds to the envelope 23 according to Wulff's theorem. Here $\dfrac{\partial^2 F}{\partial p^2} < 0$, and the curvature of the envelope is negative [see Eq. (2.1)]. At the inflection point Q_3, $\dfrac{\partial^2 F}{\partial p^2} = 0$, and the corresponding curvature of the envelope at the point 3 is infinite. The interval $Q_3 Q_6$ produces the smooth curve 36. This is followed by the inflection point Q_6 on $F(p)$ and the reversal point C on the envelope, the smooth segment 67 and the straight line 78 which is orthogonal to the radius vector 08.

The curvature of the envelope at the point with slope p is $\Omega\Lambda\left(\dfrac{\partial^2 F}{\partial p^2}\right)^{-1}$. Therefore if $F(p)$ had a sharp minimum $\left(\dfrac{\partial^2 F}{\partial p^2} = \infty\right)$ instead of a smooth minimum between Q_3 and Q_6, 36 would be a straight segment.

At the self-intersection point 4 of the envelope, the transition from 12 to 36 can be made directly, avoiding the unstable segment 23. This jump corresponds to the direct transition from Q_1 to Q_4 on $F(p)$. Analogously, the corner point 5 arises in the jump from Q_5 to infinity $\left(\varphi = \dfrac{\pi}{2}\right)$. A direct transition from 12 to 78 is theoretically possible, with the formation of the corner point C. But, by the selection rules for corner points, the contour 1C8 (the tangent $Q_1 Q_\infty$) does not provide an energy minimum. For this reason the corner point is unstable.

The equilibrium form, one corner of which is shown in Fig. 3b, corresponds qualitatively to some modification of $\alpha(p)$ (the dashed curve in Fig. 5b).

5. The Equilibrium Shape of an Open Curve

We shall determine the equilibrium profile of a crystalline surface that is unbounded in all directions, the mean slope of which does not coincide with any close-packed grid and is described by complex Miller indices[22] (such as the surface in Fig. 1).

Let us first consider the equilibrium shape of the contour between the two fixed points $A(0,0)$ and $B(l,h)$ in Fig. 6. This shape must satisfy both Eq. (2.2) and the conditions

$$y(0) = 0, \qquad y(l) = h. \tag{5.1}$$

It is convenient to replace the condition that the two-dimensional volume is constant by giving the value of the chemical potential of the medium in equilibrium with the crystal, i.e., the constant $\Lambda = \Omega^{-1}(\mu_m - \mu_{C_0})$. The relation between V and Λ is given by the form of the function $y(x, \Lambda)$ and the condition $\displaystyle\int_0^l y(x, \Lambda) = V$.

Let us first assume $\Lambda \neq 0$ ($\Lambda \gtrless 0$). The solution $y(x, \Lambda)$ must satisfy (2.2) for the two-dimensional case. Therefore we must plot a closed equilibrium contour (according to Wulff's theorem) for a given value of Λ, and insert this contour between A and B in such a way that the crystallographic orientations of the closed equilibrium shape and of the crystalline matter between A and B will coincide. $y(x, \Lambda)$ is determined from (3.3), and for $\Lambda \neq 0$ there will be a one-to-one correspondence between V and Λ. The contours a and b in Fig. 6 correspond to $\Lambda > 0$, while the contours f and g correspond to $\Lambda < 0$.

Let, now, $\Lambda = 0$, i.e., the chemical potential of the medium equals the chemical potential μ_{C_0} of an infinite crystal. In this case no closed equilibrium shape and one-to-one correspondence between V and Λ can exist. In accordance with (3.3) the smooth segments of $y(x, \Lambda)$ can only be straight lines for $\Lambda = 0$. Therefore in this case the solution of (2.2) and (1.11) must be a broken line connecting A and B, the segments of which (intersecting at the corner points) must be oriented in agreement with (3.2).

The solution with a single corner point and $\Lambda = 0$ is represented in Fig. 6 (c and e) and corresponds to unique values of the volume V.* The solution with two corner points has the form of a step; Fig. 6d corresponds to an entire interval of values of V, and as V increases or decreases this form is converted into a broken line with a single corner point. A broken line with a large number of corner points gives a stepped surface profile.

---

*The straight line AB does not give an energy minimum according to the selection rules for corner points, and is transformed into a solution such as that shown in Fig. 6d.
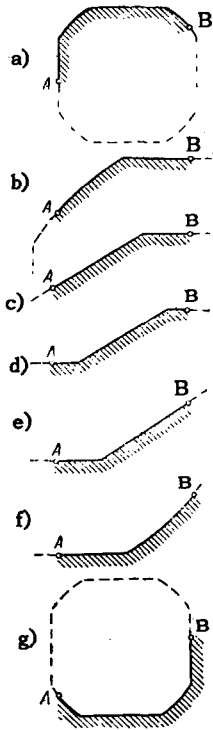
FIG. 6. Equilibrium profile of the crystal surface between the points A and B. a, b—when the chemical potential of the surrounding medium is greater than the potential of the unbounded crystal ($\Lambda > 0$); c, d, e—when $\Lambda = 0$; f, g—when $\Lambda < 0$.

It must be emphasized that, depending on the character of the anisotropy of α (p), the rectilinear segments comprising a stepped profile may or may not be close-packed.

The equililibrium shape of an <u>infinite</u> surface obeys the periodicity condition $y'(0) = y'(l)$ as well as (2.2) and (5.1). The only ones of the above-described solutions that satisfy this requirement are those with an even number of corner points for $\Lambda = 0$. Consequently, the profile of an infinite surface must consist of macroscopic steps when nontrivial solutions of (3.2) satisfy the stability conditions or, equivalently, when the equilibrium shape of a bounded two-dimensional crystal has corner points.* Otherwise the profile of an infinite surface will be a straight line. The chemical potential of the medium above a stepped surface is μC_0.

It can be shown that in the general <u>three-dimensional</u> case an infinite surface must consist of plane regions intersecting to form both edges and vertices; this also holds true for a bounded crystal with equilibrium shape.

At temperatures $T > 0$ the edges of salient corners (but not those of reentrant corners) are smeared by fluctuations. Therefore on a microscopic scale the edge of a salient dihedral edge of a step will be rounded, while the edge of a reentrant corner will be like that for $T = 0$. The same applies to vertices.

In the model under consideration the edge energy of a crystal (the intrinsic energy of corner points in the surface profile) has not been taken into account. Therefore the heights of <u>macroscopic</u> steps and the

---

*Except when $F = 1 + |p|$ and the surface is in a state of neutral equilibrium with a constant sign of p.

distances between them cannot affect the surface energy, and will thus assume any arbitrary values. The breakdown of macroscopic steps into <u>elementary</u>' steps is equivalent to the disappearance of the former and is thus not advantageous.

It was shown above that macroscopic steps can appear on a surface only when F (p) has segments of both positive and negative curvature. F (p) is determined by the energy of interaction between elementary steps on non-close-packed boundaries. In the absence of this interaction the energy is simply the sum of the energies of the close-packed segments and of the end faces (or fronts) of elementary steps, i.e., for a simple cubic lattice we have[15]

$$\alpha(\varphi) = \alpha_0(|\cos \varphi| + |\sin \varphi|), \qquad (5.2)$$

where $F = 1 + |p|$, which means that for $0 < p < \infty$ we have $\dfrac{\partial^2 F}{\partial p^2} = 0$ ($\alpha + \alpha'' = 0$). F (p) is a straight line in this case, any pair of values for p satisfies (3.2), and the contour can have any shape between A and B if the sign of p does not change. Therefore the creation of a rough stepped surface is associated <u>exclusively</u> with the departure of the asymmetry of α from (5.2).

Experiments for the determination of crystalline surface energy are known to require great accuracy and do not always permit an unambiguous interpretation. The pertinent literature is partially collected in a monograph by Kuznetsov.[24] Lemmleïn and Kliya[25-27] observed directly the change of shape of small NH_4Cl crystals that results from surface energy under isothermal conditions, and finally obtained rounded crystals.

The production of macroscopic steps by thermal etching in a vacuum has been observed by Lukirskiï,[28] Geguzin and Ovcharenko[29] for Cu, by Moor for Ag,[30] and by Young and Gwatemy for Cu.[31] However, these experiments were not performed under conditions of equilibrium. Geguzin and his co-workers have observed the production of macroscopic roughness under equilibrium conditions, at constant vapor pressure and temperature.*

II. CRYSTAL GROWTH FROM VAPOR

In this chapter we shall consider the motion of steps during growth from the gaseous phase,[14] following a brief description of the properties of adsorbed atoms and molecules.[13,14] The condition used here for particle exchange between elementary steps and an adsorbed layer leads to somewhat different expressions than those given in reference 14 for the speed of motion of an individual step, or of a group of parallel steps, and the normal growth rate determined by a screw dislocation.

We shall also discuss the kinetics of the motion of

---

*The author is indebted to Ya. E. Geguzin for the communication of unpublished results.

macroscopic steps in growth from a vapor and their stability against decay into lower steps.

6. Particles Adsorbed on a Surface

Whether a crystal is in equilibrium with the surrounding medium or not, its surface holds adsorbed particles (atoms, molecules, atomic complexes etc.) of the crystalline material (position 4 in Fig. 1). Adsorbed particles perform thermal oscillations in three directions, two of which are parallel and one perpendicular to the surface. Energy fluctuations of the perpendicular oscillations separate particles from the surface and transform them into vapor. As a result of the parallel oscillations, adsorbed atoms (or molecules) jump to neighboring positions of the two-dimensional grid, i.e., they migrate by diffusion over the surface.

The oscillatory frequency of an adsorbed particle will be denoted by ν, and its binding energy on the surface by W_s'. Then the mean lifetime of an adsorbed atom or molecule on the surface will be

$$\tau_s \sim \frac{1}{\gamma_s \nu} \exp\left(\frac{W_s'}{kT}\right), \qquad (6.1)$$

where $\gamma_s < 1$ is a coefficient associated with the necessity for surmounting the activation barrier in transitions between the adsorbed layer and the vapor. The density of adsorbed particles can be expressed by

$$n_s = n_{s_0} \exp\left(-\frac{W_s}{kT}\right), \qquad (6.2)$$

where W_s is the energy required to transfer a particle from position 3 in a kink to position 4 on the surface (Fig. 1). $n_{s_0} \sim a^{-2}$ for atoms and simple molecules, but differs from a^{-2} by an entropy factor for more complex particles (of necessarily lower concentration). Equation (6.2) reflects the possibility of particle exchange between the crystal and the adsorbed layer via kinks in a step. The value of n_s can also be derived from the condition for equilibrium between the adsorbed layer and the medium.

The energy of attachment of particles to different positions on a crystal was calculated in the classical papers by Kossel[3] and by Stranski,[4] who showed that the transition energy when an atom or molecule passes from a kink to the surrounding medium equals the heat of crystallization: $W = W_s + W_s'$.

If U_s and a are the height and width of the potential barrier between neighboring adsorption positions, the surface diffusion coefficient is

$$D_s \sim a^2 \nu \exp\left(-\frac{U_s}{kT}\right). \qquad (6.3)$$

The average path traversed by an adsorbed particle during its lifetime on the surface is

$$\lambda_s \sim (D_s \tau_s)^{\frac{1}{2}} = a\gamma_s^{-\frac{1}{2}} \exp\left(\frac{W_s' - U_s}{2kT}\right). \qquad (6.4)$$

Assuming $W_s' = W_s = \frac{1}{2}W$, $\gamma_s = 1$, $\frac{W}{kT} = 24$ (which

is a typical value when the surrounding medium is a vapor), and also, following Mackenzie,[14] that $U_s = \frac{1}{20}W$, we have

$$\lambda_s \sim a \exp\left(\frac{W_s'}{2kT}\right) \sim 4 \cdot 10^2 a.$$

The values of n_{s_0}, τ_s, λ_s, γ_s, D_s, W_s and W_s' depend on the orientation of the face to which they pertain. The crystallization energy W must, of course, be identical for all faces.

The foregoing considerations apply both to crystal-vapor and crystal-solution interfaces.

7. The Motion of an Isolated Step

Consider a crystal surrounded by a supersaturated vapor, so that its chemical potential μ_C is smaller than the gas potential μ_G. As a result of particle exchange between a step (i.e., kinks) and the adsorption layer, extra particles join the crystal at the kinks, and the value of the chemical potential of adsorbed particles (and vapor) around the step is close to μ_C. Therefore diffusion begins in the vapor and adsorbed layer in the direction of the step, on which crystallization will be continuous so long as supersaturation is maintained.

Few particles reach the end-face of a step directly from the vapor because of low vapor pressure and small end-face area. This circumstance induced Volmer[32] to suggest an adsorbed layer in order to interpret experiments on mercury platelet growth from a vapor. The principal contribution therefore comes from a two-dimensional diffusion current of atoms or molecules adsorbed on close-packed portions of the surface, where particles cannot make the transition to the crystalline phase. The area of these regions is large, and a considerable number of particles is deposited upon them in unit time before diffusing to the step.

Let us consider the motion of an elementary step, assuming that matter reaches its end-face only by two-dimensional diffusion. In view of the subsequent investigation of macrostep motion, it is more convenient to employ, instead of the density n_s of adsorbed particles, their chemical potential μ, which under conditions of equilibrium is independent of face orientation.

The current of adsorbed particles on the surface is given by

$$\mathbf{j}_s = D_{\mu s} \nabla \mu, \qquad (7.1)$$

where $D_{\mu s} = \left(\frac{\partial n_s}{\partial \mu}\right)_{T,P} D_s$ and the gradient ∇ is taken along the crystal surface. In first approximation the current from the gas to the surface is

$$j_v = \gamma (\mu_G - \mu), \qquad (7.2)$$

where

$$\gamma = \frac{1}{\tau_s} \left(\frac{\partial n_s}{\partial \mu}\right)_{T,P}.$$

Since the motion of a step is considerably slower[14] than the characteristic diffusion rate D_S/λ_S, the step can be regarded as fixed in solving for the diffusion of adsorbed particles. In this approximation the matter conservation law div $j_S = j_V$, in conjunction with (6.1), (6.4), and (7.2), gives

$$\lambda_s^2 \Delta\mu - (\mu - \mu_0) = 0. \qquad (7.3)$$

When the step is parallel to the z axis, we have $\mu = \mu(x)$. The step can be regarded as a line sink for adsorbed particles. It is reasonable to assume that the strength of this sink is proportional to the departure from the equilibrium chemical potential of the immediately surrounding particles. Therefore on the step $(x = 0)$

$$D_{\mu s}\left\{ \frac{d\mu}{dx}\Big|_{x=0+0} - \frac{d\mu}{dx}\Big|_{x=0-0} \right\} - \beta_\mu(\mu(0) - \mu_C) = 0, \qquad (7.4)$$

where β_μ is a coefficient characterizing the rate of particle exchange between the step and adsorbed layer. β_μ obviously characterizes only the step and does not depend on the distribution of diffusion currents in the system. β_μ is also smaller than the density of kinks in the step.

Burton, Cabrera, and Frank[14] used, instead of (7.4), a somewhat different condition, which for the chemical potential $\mu(0)$ of particles adsorbed near the step is given by

$$\mu(0) - \mu_C = (1 - \beta^*)(\mu_G - \mu_C). \qquad (7.5)$$

Here the dimensionless coefficient β^*, like β_μ in (7.4), reflects the necessity of a finite relaxation time τ before equilibrium is established between the crystal and adsorbed layer near the step. Since it relates supersaturation around the step, $\mu(0) - \mu_C$, with supersaturation $\mu_G - \mu_C$ in the vapor far from the step, the coefficient $\beta^* = \left(1 + \dfrac{\lambda_S \tau}{a\tau_S}\right)^{-1}$ must depend on the geometry of the diffusion field. In reference 14, however, it was regarded as constant.

In solution of (7.3) with the boundary condition (7.4) at $x = 0$, and $\mu = \mu_G$ at $x = \pm\infty$, is

$$\mu(x) = \mu_G - (\mu_G - \mu_C)\left(1 + \frac{2D_{\mu s}}{\lambda_s \beta_\mu}\right)^{-1} \exp\left(\mp \frac{x}{\lambda_s}\right). \qquad (7.6)$$

The negative sign pertains to the region $x > 0$, and the positive sign to $x < 0$. The velocity of step motion is thus

$$v = 2a^2 D_{\mu s}\left[\frac{d\mu}{dx}\right]_{x=0} = \frac{2a^2 D_{\mu s}}{\lambda_s}(\mu_G - \mu_C)\left(1 + \frac{2D_{\mu s}}{\lambda_s \beta_\mu}\right)^{-1}. \qquad (7.7)$$

If P_0 is the equilibrium vapor pressure above the crystal, and P is the actual vapor pressure, then for small departures from equilibrium we have

$$\mu_G - \mu_C \cong kT \frac{P - P_0}{P_0} \equiv kT\sigma. \qquad (7.8)$$

Using (6.1) — (6.4) and (7.8), we obtain from (2.11)

$$v = 2\sigma\gamma_s\lambda_s v \exp\left(-\frac{W}{kT}\right)\left(1 + \frac{2D_s}{\lambda_s\beta}\right)^{-1}. \qquad (7.9)$$

$\beta = \beta_\mu\left(\dfrac{\partial n_s}{\partial\mu}\right)_{T,P}$ can be represented by a/τ, where τ is the aforementioned relaxation time. For the factor playing the part of β^* here we now have

$$\left(1 + \frac{2D_s}{\lambda_s\beta}\right)^{-1} = \left(1 + \frac{2\lambda_s\tau}{a\tau_s}\right)^{-1},$$

which agrees with the expression for β^* in reference 14 within a factor of 2. The velocity (7.9) of an isolated step is independent of the crystallographic orientation of the step, being determined by the isotropic diffusion current. Anisotropy of v can result from anisotropy of the two-dimensional diffusion coefficient D_S and of β.

8. Parallel Sequences of Elementary Steps

Let an infinite sequence (or "staircase") of parallel elementary (unit) steps exist. If the separation of neighboring steps is $\lambda \lesssim \lambda_S$ their diffusion fields overlap, and the speed of motion will diminish as λ decreases. The speed of step motion in a sequence, calculated by analogy with that of an isolated step (Sec. 7), is

$$v = 2\sigma\gamma_s\lambda_s v \exp\left(-\frac{W}{kT}\right)\left(1 + \frac{2\lambda_s}{\beta\tau_s}\,\mathrm{th}\,\frac{\lambda}{2\lambda_s}\right)\mathrm{th}\,\frac{\lambda}{2\lambda_s}. \qquad (8.1)^*$$

Equations (7.9) and (8.1) contain the dependence of step velocity on their curvature k if the radius of curvature is $1/k \gg \lambda_S$. Indeed, $\mu_K = \mu_{K_0} + \Omega\alpha k$ when α is isotropic, and

$$\mu_G - \mu_C = (\mu_G - \mu_{C0})\left(1 - \frac{\Omega\alpha k}{\mu_G - \mu_{C0}}\right) = kT\sigma(1 - k\varrho_c),$$

where $\rho_C = \dfrac{\Omega\alpha}{\mu_G - \mu_{C_0}}$ is the critical radius of curvature of a two-dimensional nucleus under supersaturation $\mu_G - \mu_{C_0}$. Hence,

$$v = v_0(1 - k\varrho_c). \qquad (8.2)$$

For an isolated step v_0 is given by (7.9), and for a step in a sequence by (8.1). Portions of a step with curvature $k > 1/\rho_C$ will dissolve, rather than grow, under supersaturation. When $k = 1/\rho$ we have $v = 0$.

9. The Normal Rate of Spiral Growth

The motion of steps regardless of their source has been considered in Secs. 7 and 8. In the classical theory[2-10] the sources of steps are two-dimensional nuclei formed on close-packed crystal faces. However, the probability of the formation of these nuclei on unit surface area in unit time is proportional to

$$\exp\left\{-\frac{\pi\Omega a\alpha^2}{kT(\mu_G - \mu_C)}\right\}, \text{ and attains an appreciable}$$

*th = tanh.

value only at supersaturations $\sim 50\%$, while for
smaller departures from equilibrium there will be
practically no growth. Crystals actually grow at the
easily measurable rates of $10^{-5} - 10^{-4}$ cm/sec at
supersaturations $\lesssim 1\%$. This contradiction between
theory and experiment was accounted for in 1949 by
Frank, who pointed out that a surface intersected by
a screw dislocation acquires a step, equal in height
to the projection of the Burgers vector of the disloca-
tion on the normal to the surface, which does not dis-
appear during the growth process (Fig. 7). Growth at
dislocations can proceed even under low supersatura-
tion; therefore it becomes unnecessary to regard the
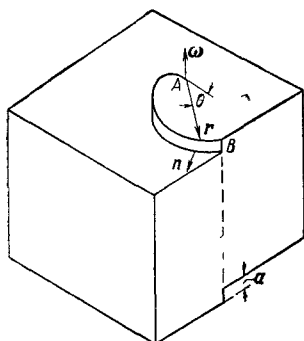growth rate as limited by the nucleation rate.

FIG. 7. A screw dislocation in a crystal and the initial aevel-
opment of a spiral step ω — angular rate of spiral "rotation";
n — normal to step (in close-packed plane). The Burgers vector a
has the same direction as ω and is equal in magnitude to the
height of the step resulting from incomplete slip in the crystal.

A crystal containing one screw dislocation con-
sists, if the lattice is simple, of a single helicoidal
atomic layer. The step, which terminates on the sur-
face at the emergence point of the dislocation, grows
spirally around that point as a center. Heck[33] ob-
served the typical spiral on paraffin crystals as early
as 1937, but the significance of his observations was
not duly appreciated. In 1945 Lemmleïn[34] rediscovered
the spiral topography, on the basal face of a SiC crys-
tal. X-ray studies of polytypism by Zhdanov and Miner-
vina[35] at about the same time enabled Lemmleïn to de-
termine the relationship between the spiral topography
of the face and the helicoidal-polytypic structure of
silicon carbide crystals.* At that same time Lemmleïn
spoke of spiral centers as continuous sources of
layers.[34]

However, an intensive study of the spiral topogra-
phy began only after the publication of Frank's paper,[12]
when the significance of dislocations for growth under
low supersaturation was understood. The spiral pattern
was observed on a huge number of crystals grown from
vapor[34,36,37] and from solution,[39] on a much smaller
number grown from the melt,[40] and in electrolytic
growth.[41,43] Spirals generated by dislocations have

*Polytypism has been discussed in the books by Varma[44] and
by Amelinckx and Dekeyser,[37] and in Mitchell's review article.[45]

been observed on crystals with different types of bonds,
lattice structure, and symmetry.

At the present time it can be asserted confidently
that spiral growth, if it is not the only form of growth
in conditions of low supersaturation, must, in any
event, be regarded as quite typical and universal.

Let us consider the formation of a spiral growth
pattern, and determine the normal growth rate of a
face resulting from a screw dislocation. Let the crys-
tal exhibit a rectilinear elementary step AB (Fig. 7),
where A is the emergence point of the screw disloca-
tion. During growth all points except A begin to move
with the same linear velocity v along the normal to
AB. Thus the entire step acquires a spiral form and
a "hill" grows on the face of the crystal.

In growth the spiral "rotates" around the point A
with the angular velocity $\omega \cong \dfrac{v_0}{2\rho_c}$, where v_0 is given
by (8.1), and the separation of adjacent turns is

$$\lambda = 4\pi\varrho_c, \tag{9.1}$$

since the spiral is represented by $r = 2\rho_c\theta$ in polar
coordinates (r, θ). A more accurate calculation some-
what reduces ω (Fig. 22),[46] and $\lambda \cong 19\rho_c$.

The foregoing expressions for the shape of a spiral
and for its velocity of "rotation" on a crystal surface
depend on the mechanism for step motion only through
v_0, and, depending on the specific form of v_0, are ap-
plicable to growth from a vapor, solution, or melt. In
the given model the separation λ between successive
turns is entirely independent of the growth mechanism
and depends only on supersaturation (or undercooling).
Using (9.1) and (8.1), we obtain the normal rate for a
face that is determined by a dislocation with a screw
component of the Burgers vector equaling the inter-
atomic spacing a:

$$V = \frac{a}{\lambda}\, v = \gamma_s a v \sigma_c \exp\left(-\frac{W}{kT}\right)$$

$$\left\{\left(1 + \frac{2\lambda_s}{\beta\tau_s}\text{th}\,\frac{\sigma_c}{\sigma_1}\right)^{-1}\left(\frac{\sigma}{\sigma_c}\right)^2\text{th}\,\frac{\sigma_c}{\sigma}\right\}, \tag{9.2}$$

where

$$\sigma_c \equiv \frac{2\pi\Omega a}{kT\lambda_s}.$$

With $\sigma \ll \sigma_c$, when the turn separation of the spiral
is $\lambda \gg \lambda_s$, the diffusion fields of the turns do not over-
lap, and $V \sim \sigma^2$. If $\sigma \gg \max\left\{\sigma_c, \dfrac{\lambda_s}{\beta\tau_s}\sigma_c\right\}$, then
$V \sim \sigma$. When β is much smaller than the character-
istic surface diffusion rate λ_s/τ_s, a linear segment
can be initiated only at extremely high supersatura-
tions.

Equation (9.2), which is basically the same as the
corresponding expression in reference 14, differs
from the latter in the presence of the denominator
$\left(1 + \dfrac{2\lambda_s}{\beta\tau_s}\tanh\dfrac{\sigma_c}{\sigma}\right)^{-1}$ depending on supersaturation,
and also because under high supersaturation the role

of β^* in reference 14 is here played by the coefficient γ_s, which is related to the relaxation time required to establish equilibrium between the adsorbed layer and the vapor (rather than the step, as in reference 14).

The function $\dfrac{V \exp\left(\dfrac{W}{kT}\right)}{a \nu \gamma_s \sigma_c}$ has been plotted in Fig. 8

for $\dfrac{2\lambda_s}{\beta \tau_s} = 0$ and 1, $\sigma_c = 0.1$, which are obtained from the relaxation time $\tau \cong \dfrac{1}{\nu} \exp\left(\dfrac{W}{4kT}\right)$ with the following numerical values: $kT = 5 \times 10^{-14}$ erg, $\alpha = 3 \times 10^2$ erg/cm^2, $\lambda_s = 4 \times 10^2 \times 3 \times 10^{-8}$ cm, and $\Omega = 3 \times 10^{-23}$ cm^3.
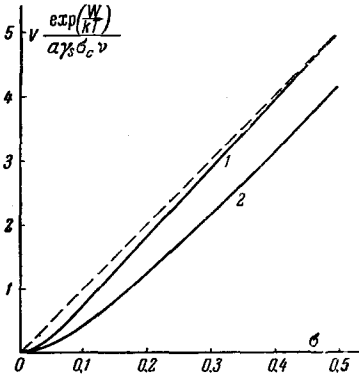

FIG. 8. Normal rate of dislocation-induced growth of a face as a function of supersaturation [Eq. (2.14)]. Curve 1 — for $\dfrac{2\lambda_s}{\beta \tau_s} = 0$,

curve 2 — for $\dfrac{2\lambda_s}{\beta \tau_s} = 1$. For smaller β curve 2 can be considered to to be the function V(σ) in the presence of impurities.

10. The Motion of Macroscopic Steps

We shall now investigate the motion of macroscopic steps, the shape and very existence of which in conditions of crystal-medium equilibrium is determined by the anisotropy of the surface specific energy (Ch. I).

When the end face of a step is a close-packed macroscopic crystal face, crystallization upon it is possible only through the motion of steps. When dislocations do not emerge on the end face, the sources of steps must be nuclei, which can be formed most easily at the edge of a reentrant corner such as CC' (Fig. 9). If the height of a macroscopic step is smaller than the radius of the critical nucleus, the latter cannot appear on the end-face of the macrostep. Therefore the macrostep will move only at supersaturations

$$\sigma > \sigma^* = \frac{\Omega \alpha \sin \varphi_0}{kTh}.$$

With increasing step height $h > \dfrac{\Omega \alpha \sin \varphi_0}{kT\sigma}$, the step velocity must increase because of higher nucleation probability.

The end surface of a step will not necessarily be close-packed (Sec. 3). Moreover, if the step height is of the order of tens of interatomic spacings or less,
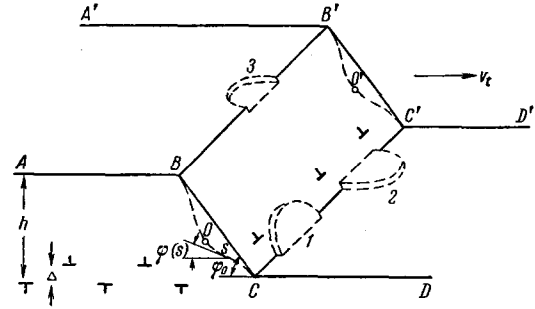

FIG. 9. A macroscopic step in conditions of equilibrium (solid lines); distortion of its end-face BB'C'C in growth (dashed curves). 1 and 2 are nuclei of new growth monolayers; 3 is an evaporation nucleus. The edge BB' and part of the end-face can in actuality be smeared out by fluctuations.

the end surface is subject to fluctuation smearing. In such cases an appreciable number of kinks is found in the end-face, and the nucleation stage does not limit the rate of the growth process. Of primary importance, however, is the rate at which the end-face is supplied with crystallizing matter — an aspect that we have lately been considering.[22,23] It is reasonable to assume that adsorbed particles migrate over both close-packed and non-close-packed surface regions, but with different diffusion coefficients. In conditions of equilibrium let the end surface make the angle φ_0 with a close-packed face (Fig. 9), and in the growth let it move at velocity V_t and assume a stationary form represented by $\varphi(s)$, where s is the length along the surface profile measured from the point O. The condition for a stationary profile of the end-face will be

$$\Omega \beta_\mu [\mu(s) - \mu_c] = V_t \sin \varphi. \qquad (10.1)$$

The chemical potential μ (s) of adsorbed particles obeys the equation

$$\frac{d}{ds}\left(D_{\mu s} \frac{d\mu}{ds} \right) - \gamma_\mu(\mu - \mu_c) - \beta_\mu(\mu - \mu_c) = 0. \qquad (10.2)$$

The second term describes flow from the gas to the adsorbed layer, while the third term describes that from the adsorbed layer to the crystal. The coefficients $D_{\mu s}$, γ_μ, and β_μ depend generally on φ. From (2.1) we have

$$\mu_c = \mu_{c0} + \Omega(\alpha + \alpha'') \frac{d\varphi}{ds}. \qquad (10.3)$$

On the close-packed faces ABB'A' and CDD'C' (Fig. 9). $\alpha + \alpha'' = \infty$ and $\varphi = $ const $= 0$.

The orientation of ABCD to the left and right of the corner points B and C will, as in the case of equilibrium, be given by $\varphi = 0$ and φ_0, and migrating particles will flow continuously through BB' and CC'. In addition, $\mu(\pm\infty) = \mu_G$. These boundary conditions, together with (10.1), (10.2), and (10.3), determine the unknown functions $\varphi(s)$ and $\mu(s)$ and the velocity V_t of an isolated macroscopic step.

The solution of our problem in first approximation with respect to σ is

$$V_t = f(h)\,\Omega\beta_\mu\,(\mu_G - \mu_{C0})$$

$$\equiv \operatorname{cosec}\varphi_0\left[1 + \frac{\beta}{\gamma} + \frac{\beta\lambda_1}{\gamma s_0}\frac{\operatorname{sh}\dfrac{s_0}{\lambda_1}}{\dfrac{\lambda_1}{\lambda_0}\operatorname{sh}\dfrac{s_0}{\lambda_1} + \operatorname{ch}\dfrac{s_0}{\lambda_1}}\right]^{-1}, \qquad (10.4)*$$

$$\varphi(s) = \varphi_0 + A\left(\operatorname{sh}\frac{s}{\lambda_1} - \frac{s}{s_0}\operatorname{sh}\frac{s_0}{\lambda_1}\right),$$

$$A = \frac{V_t\lambda_1}{\Omega^2\gamma_\mu(a + a'')_0}\left[\operatorname{ch}\frac{s_0}{\lambda_1} + \frac{\lambda_1}{\lambda_0}\operatorname{sh}\frac{s_0}{\lambda_1}\right]^{-1}, \qquad \lambda_0 = \frac{D_0}{\gamma}, \quad \lambda_1 = \frac{D_1}{\gamma},$$

$$(10.5)*$$

where $s_0\sin\varphi_0 = h/2$ is the half-height of the step, D_0 is the diffusion coefficient over close-packed faces, and D_1 is the diffusion coefficient on the end face of the step.

The step profile corresponding to (10.5) is represented in Fig. 9 by a dashed curve. During growth the end-face "sags" and, because $\varphi(s) - \varphi_0 = -(\varphi(-s) - \varphi_0)$ (Fig. 10, curve 1), the points B and C occupy the relative positions as in equilibrium, i.e., the slope of the straight line is φ_0, as previously. When $s_0 \ll \lambda_1$,
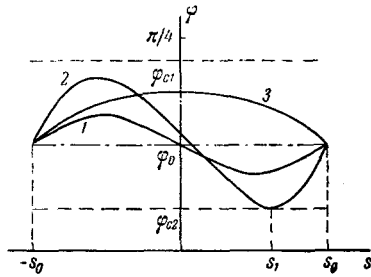

FIG. 10

the absolute value of the maximum deviation of φ from its equilibrium value is

$$|\varphi - \varphi_0|_{\max} \sim V_t s_0^3, \qquad (10.6)$$

and we have the function, decreasing monotonically with height,

$$f(h) \cong \operatorname{cosec}\varphi_0\left(1 + \frac{\beta h}{2\gamma\lambda_0\sin\varphi_0}\right)^{-1}. \qquad (10.7)$$

The "sagging" of the step profile (Fig. 9) results from the fact that the regions around B′ and C′ are better supplied with migrating particles than is the central zone around O′. The warping of the profile and the change of the supplementary chemical potential that is associated with surface energy compensate the nonuniform supply. In the absence of surface energy the end-face region around C′ would move faster than the central region, and the step would be unstable and smeared, becoming a non-steep sequence of elementary steps.† It follows from Sec. 4 that the step shape will be stable only if $\alpha + \alpha'' > 0$ everywhere on the end face. If kinetic processes result in orientations on the end face of the step for which $\alpha + \alpha'' < 0$,

---

*sh = sinh, ch = cosh

†A high velocity around BB′ would lead to the formation of a layer overhanging the surface.

on these regions the surface energy will not favor stability and the step will disintegrate. For example, let a random deviation MLN (the dotted line in Fig. 11) arise in the profile of a step. Then because of the deviation $\delta\dfrac{d\varphi}{ds}$ of surface curvature and the effect of surface energy, the speed of the step on MLN will change, in accordance with (10.1) and (10.3) by the amount

$$\sin\varphi_0\delta V_t = -\Omega\beta(a + a'')\,\delta\frac{d\varphi}{ds}.$$

(The redistribution of diffusion currents which is associated with the deviation MLN has not been taken into account, and $\alpha + \alpha''$ is taken to be constant.) When $\alpha + \alpha'' > 0$ the sign of δV_t is opposite to that of $\delta\dfrac{d\varphi}{ds}$, so that a random modification of the stationary shape tends to disappear. On the other hand, when $\alpha + \alpha'' < 0$, a random deviation will be augmented so that segments with $\alpha + \alpha'' < 0$ disappear.
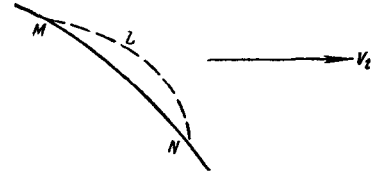

FIG. 11

Let φ_{c_1} and φ_{c_2} be values of φ at which the sign of $\alpha + \alpha''$ changes. It follows from the preceding discussion that a step will be stable at supersaturations and macroscopic step heights where

$$\min_{-s_0 < s < s_0}\varphi(s) > \varphi_{c_2}, \qquad \max_{-s_0 < s < s_0}\varphi(s) < \varphi_{c_1}, \qquad (10.8)$$

i.e., when $\varphi(s)$ (Fig. 10) remains within the strip bounded by the straight lines $\varphi = \varphi_{c_1}$ and $\varphi = \varphi_{c_2}$. With rising supersaturation the maximum departure of $\varphi(s)$ from its equilibrium value φ_0 increases, and the symmetry of $\varphi(s)$ will generally be destroyed because of higher-order supersaturation terms, and also because the end-face of the step is not built up uniformly from the gaseous phase (Fig. 10, curve 2). Therefore the curve of $\varphi(s)$ can first touch either $\varphi = \varphi_{c_2}$ or $\varphi = \varphi_{c_1}$. In the first case the macrostep at the point s_1 divides into two steps with the heights $(s_0 + s_1)\sin\varphi_0$ and $(s_0 - s_1)\sin\varphi_0$. The latter, being lower, has a higher velocity and will overtake the former. Therefore, with rising supersaturation the original macrostep will break down until it reaches a height for which (10.8) is fulfilled. Using (10.6) for a tentative estimate, we find that at any given supersaturation the only stable steps will have heights obeying

$$h < h_c\mathrm{const}\cdot\sigma^{-1/3}. \qquad (10.9)$$

It must be remembered that steps resulting from

the foregoing separation process are also macroscopic, like the initial step.

If with rising supersaturation the second condition in (10.8) is violated first, a macroscopic layer will appear above the surface; this is essentially a lamellar dendritic crystal.

The described mechanism of macroscopic step breakdown comes into operation only when the supersaturation exceeds a critical value corresponding to the step height.

It follows from (10.9) that $h_c \sim \sigma^{-1/3}$, thus diminishing quite slowly as the supersaturation rises. At high supersaturations a second mechanism of macroscopic step decay becomes effective. This involves the <u>nucleation</u> of elementary steps at a reentrant corner such as CC' (2 in Fig. 9). When this process begins to become intense, the mean step height on the surface drops sharply to the order of a few lattice parameters. Under such degrees of supersaturation macroscopic steps can arise and remain stable for purely kinetic reasons alone (Ch. VI). For example, an annular macroscopic step can arise around a screw dislocation if the stream intensity of elementary steps separated from the macroscopic step is less than that emitted by the dislocation (see Sec. 11, Fig. 13d).

Let us imagine two surfaces with identical orientations but different mean step heights $\bar{h}$. On the surface with greater step height the mean step separation $\bar{\lambda}$ is greater. If on this surface $\lambda \gtrsim \lambda_s$, step breakdown under the same supersaturation will lead to an increased normal rate of growth. Indeed, $V \sim (\bar{h}/\bar{\lambda}) f(\bar{h})$, and, if $\bar{h} \sim \bar{\lambda}$, then $V \sim f(h)$. The surface with lower step height uses the current from the gaseous phase "more efficiently."

The sole cause of macroscopic step stability considered in this section has been the anisotropy of surface energy. Kinetic processes, on the contrary, tended to destroy macrosteps by converting them into sequences of elementary steps. However, it is possible to have kinetic factors that promote the relative stability of a step (see Secs. 18 and 22, for example).

11. Some Experimental Results

The quadratic form of $V(\sigma)$ for $V \lesssim 1\%$ is indicated by the data in the paper of Volmer and Schultze[48] on the growth of iodine crystals from vapor.

A distinctly nonlinear form of $V(\sigma)$ was obtained from measurements of the normal growth rate of an individual spiral hill on crystals of β-methyl naphthalene and p-toluidine (Fig. 12) grown from vapor with $5\% \lesssim \sigma \lesssim 80\%$. The normal growth rate in this case depends on the screw component of the Burgers vector of the dislocation that generates the hill (curves 1, 2, and 3 in Fig. 12).

The shape of the $V(\sigma)$ curve is correlated with the stepped structure of the surface. The transition from a nonlinear to a linear segment of $V(\sigma)$ is character-
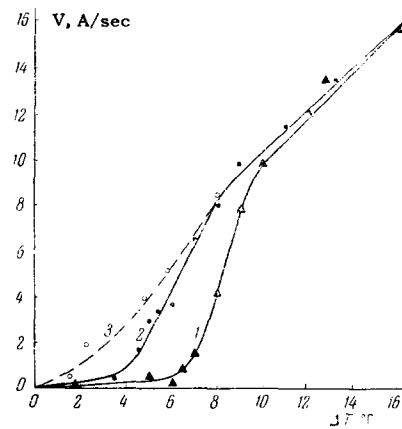

FIG. 12. Normal rate of spiral growth from vapor on the (001) face of a β-methyl naphthalene crystal. The Burgers vector for 1 is 4c; for 2 it is 40c and for 3 it is 60c. The lattice constant along the c axis is 23.5 A.

ized by supersaturation at which direct microscopic observation of the intense decay of high steps is possible. Figures 13a — d shows successive stages of the disintegration of a spiral step as supersaturation rises. The first two photographs show the breakdown of a spiral macrostep to form macroscopic steps that are visible microscopically. At supersaturation $\sigma \sim 40\%$ intense decay of the spiral layer begins, with the apparent creation of low steps that are not microscopically distinguishable. The visible spiral disappears,
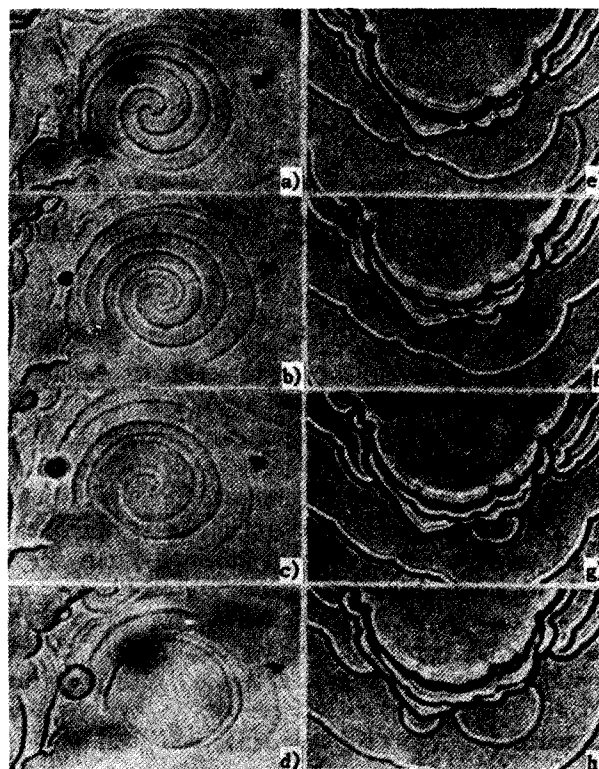

FIG. 13a–d). Disintegration of a spiral step as supersaturation increases. e–h) Disintegration of a layer with the emission of a macroscopic step (indicated by arrows).

and a high circular step appears around its former center (Figs. 13e — h). $\sigma \sim 50\%$ corresponds to the beginning of the linear segment of $V(\sigma)$. If the supersaturation is now lowered, a growth spiral reappears at the previous site. One possible cause of the observed nonlinearity of $V(\sigma)$ is the disintegration of steps discussed in Sec. 10 and the increase of their mean density with rising supersaturation.

Successive motion-picture frames in Figs. 13e — h show the disintegration of a macroscopic step with the evolution of another, lower, macrostep.[49] This process was photographed at <u>constant</u> supersaturation.

The decrease of step velocity as height increases has been noted qualitatively by many authors, and specifically in reference 50 for growth from a solution. Quantitative measurements of $f(h)$ in growth from vapor have been performed by Lemmleïn and Dukova,[51] and by Kozlovskiĭ[52] on crystals of p-toluidine and β-methyl naphthalene. These data agree satisfactorily with $f(h)$ in (10.7) when h is smaller than λ_1, the mean free path of an adsorbed particle on the end face of a step.[53] When $h \gtrsim 0.1$ micron the measured velocity of an end face approaches asymptotically a value close to the velocity of the corresponding macroscopic face.

12. Evaporation*

The discussed molecular kinetic ideas concerning the motion of elementary steps can obviously be applied completely to the case of evaporation, i.e., negative values of σ. In evaporation, steps move in the opposite direction, and depressions, instead of hills, are formed at dislocations. Within the framework of the ideas already developed regarding the role of surface energy in the lifetime of macrosteps, their velocity and shape can be derived from (10.4) and (10.5) by the substitution $\sigma \rightarrow -\sigma$. If, however, the edge BB' of a salient dihedral corner is extremely smeared by fluctuations, the splitting-off of elementary steps does not necessarily require nucleation, and will proceed more intensely and at lower values of σ than for growth. Similarly, a crystal edge will serve as a source of steps in evaporation. This hypothesis has been corroborated experimentally by Hirth and Pound[54] and by Sears.[55] When a narrow (~ 1 micron) microjet of undersaturated vapor impinged on the edge of a crystal plate of para-toluidine, Sears observed the splitting of layers from this edge, whereas a stream directed at the middle of a perfect crystal did not cause evaporation of the latter.

According to reference 54 the separation of elementary steps is $\sim 6\lambda_S$ when they are far removed from the emitting edge. Unfortunately, it has not been possible to repeat the calculations in reference 54 pertaining to the distribution of steps near the crystal edge. Frank[56] has presented a phenomenological theory of the surface profile near an edge during

*See also Ch. V, "Etching."

evaporation, without account of surface energy (see Sec. 22).

III. CRYSTAL GROWTH FROM THE SOLUTION AND FROM THE MELT

13. Introduction

Crystals are usually grown in practice from the liquid phase — either the solution or the melt. Crystallization from the condensed phase has been studied in a large number of special investigations, but the mechanism of growth, especially from the melt, is at present much less well understood than that from the vapor.

The rate of crystal growth from the gaseous phase is not limited by mass transfer in the vapor, since such transfer proceeds quite rapidly, at least in the case of a pure gas. When the feeding of the growing crystal is impeded by the presence of a gaseous impurity or by a solvent (in growth from the solution), mass transfer in the body can proceed more slowly than the diffusion of adsorbed particles on the crystal surface; this circumstance must not be neglected. Thermal conduction must also be considered in growth from the melt, and sometimes in growth from the solution.

We shall consider growth from the solution first. If the entire solution is motionless and of sufficiently large volume, the growth rate will be limited by the diffusion resistance of the solution, which is directly proportional to the linear size of the space occupied by the solution, and is inversely proportional to the diffusion coefficient. If the solution is stirred, pure diffusion transfer (without hydrodynamical transfer) actually occurs nowhere. However, it may be assumed approximately that a thin layer of liquid remains motionless at the liquid-crystal interface, and that the diffusive transfer of dissolved matter takes place through this layer.

In the original version of the diffusion theory of growth[57,58] the concentration of the solution at the crystal surface was taken to be its equilibrium value at the given temperature. This simplest isotropic model cannot account for the different growth rates of different faces. It was subsequently[59] suggested that the concentration in the boundary layer at the interface differs from the equilibrium value and varies on different faces depending on the properties of the latter. Bravais long ago,[60] and Niggli fifty years later,[61] developed the idea of a relationship between the growth rate of a face and its reticular density. These views regarding the role of the reticular density were developed further by Kossel[3] and by Stranski,[4] who analyzed the activities of different atomic sites on several crystal faces and showed that steps and kinks must exist for crystal growth. The sources of steps in growth from the solution or melt, as in the case of growth from the vapor, are either two-dimensional nuclei or dislocations. The dislo-

cation model of growth from the solution and its employment in analyzing growth from the melt[62] lead, as for growth from the vapor, to a normal growth rate V of a face that is quadratically dependent on supersaturation or undercooling σ at low values of these quantities. This conclusion can be reached regardless of the detailed mechanism and velocity of advance of each step (Sec. 9). A more detailed analysis requires the calculation of the temperature and concentration near the stepped surface; this is performed in the present section.[63] These effects yield a function $V(\sigma)$ that, over a wide range of σ, is well approximated by $M\sigma^m$, where m ~ 1.6 — 1.8, but that becomes linear for larger values of σ, so that the corresponding straight line in the (V, σ) plane does not pass through the coordinate origin. The diffusion field, rate of advance, edge shape, and stability of macroscopic steps are calculated in Sec. 15.

The foregoing discussion of growth also applies to dissolution and etching, although certain new effects also arise, such as the more intense decay of macroscopic steps (Sec. 12 and Ch. VII) and nucleation at sites with enhanced energy.

14. The Motion of a Parallel Sequence of Elementary Steps

We now consider the motion of parallel elementary steps. Let us assume, as in Sec. 2, that matter is transferred to the crystal only on the end faces of steps and only by diffusion within the volume of a fixed boundary layer of thickness δ adjacent to the crystal, i.e., the flow of adsorbed particles on the crystal toward the steps can be neglected compared with the direct flow from the solution. Estimates of the relative roles of these currents[14] unfortunately do not furnish a unique criterion for the applicability of the hypothesis in question. We shall assume, finally, that the rate of advance of steps is considerably slower than the characteristic diffusion rate in the solution (D/δ). With the diffusion coefficient D ~ 10^{-5} cm^2/sec and δ ~ $10^{-4} - 10^{-5}$ cm this inequality is well satisfied.

We denote the concentration of the solution at the edge of the boundary layer by c_δ, the height of each step by a, and the distance between steps by λ (Fig. 14). The z axis coincides with one of the steps, and the (x, y) plane intersects the crystal surface along the x axis on the average. Since step motion can be neglected in the diffusion problem, the concentration c (x, y) of the solution obeys Laplace's equation $\Delta c = 0$ everywhere in the boundary layer, while on a step, which we assume to be a semicylinder of radius a, it satisfies

$$D \frac{\partial c}{\partial r} = \beta (c - c_e) \quad \text{for} \quad r = a \quad (r = \sqrt{x^2 + y^2}). \quad (14.1)$$

Here β characterizes the rate of particle exchange between a step and the solution, diminishing as the number of kinks in the step decreases.
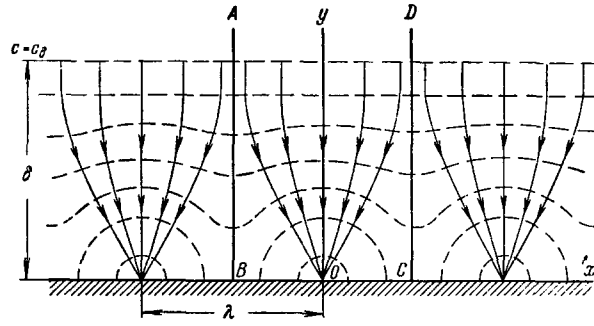

FIG. 14. Diffusion field near the stepped surface of a growing crystal. The steps are perpendicular to the plane of the figure and intersect it at the points x = 0, ± λ, ± 2λ ..., y = 0.

At the assumed limit of the boundary layer, y = δ, we have c (0, δ) = c_δ. There is no flow through the contour ABOCD, i.e., on this contour $\frac{\partial c}{\partial n}$ = 0, the derivative being taken normal to the contour.

By conformal mapping of the half-strip $-\lambda/2 \leq x \leq \lambda/2$, y > 0 on the upper half-plane, we obtain the following distribution for the concentration of the solution in the interval $-\lambda/2 \leq x \leq \lambda/2$:

$$c(x, y) = A \ln \sqrt{\sin^2 \frac{\pi}{\lambda} x + \text{sh}^2 \frac{\pi}{\lambda} y} + B, \quad (14.2)$$

where

$$A = \frac{\beta a (c_\delta - c_e)}{D + \beta a \ln \frac{\lambda}{\pi a} \text{sh} \frac{\pi}{\lambda} \delta}, \quad \beta = c_\delta - A \ln \text{sh} \frac{\pi}{\lambda} \delta.$$

Hence the velocity of advance of elementary steps in the sequence is

$$v = \pi \Omega \beta (c - c_e) = \frac{\pi \Omega \beta c_e \sigma}{1 + \frac{\beta a}{D} \ln \frac{\lambda}{\pi a} \text{sh} \frac{\pi}{\lambda} \delta}, \quad (14.3)$$

where $\sigma = \frac{c_\delta - c_e}{c_e}$, and Ω is the specific volume of a molecule (or atom) in the crystal.

In deriving (14.2), and thus (14.3), the boundary condition c (0, δ) = c_δ was used, although in actuality a boundary condition would be required along the entire straight line y = δ as well as at the point (0, δ) in the (x, y) plane. However, when $\pi\delta \gg \lambda$, for large y we find that c (x, y) is practically independent of y, and the condition used at the point (0, δ) is equivalent to a condition along the line y = δ: When $\pi\delta \ll \lambda$ it is required, from a rigorous point of view, that we use the conformal mapping, by the Schwarz-Christoffel integral, of the rectangle ABCD on the upper half-plane, rather than of the half-strip. However, for $\pi\delta \ll \lambda$ steps exist which are actually isolated from each other. Therefore near each such step the concentration can be represented approximately by

$$c(r) = A \ln r + B,$$

where A and B are derived from the conditions c (δ) = c_δ and (1.41). Then B = c_δ – A ln δ, and A and v

coincide with the expressions obtained from (14.2) and (14.3) when $\delta/\lambda \to 0$.

From the foregoing considerations we can expect that (14.3) with $\pi\delta \ll \lambda$ will hardly result in a greater error than the original physical assumptions.

15. The Normal Growth Rate

The distance λ between steps depends on the strength of the step source. A screw dislocation produces a spiral step. Far from the center of a spiral, where the radius of step curvature considerably exceeds the distance between steps, the rate of advance, as in the case of straight steps, is given by (14.3). Near the center of the spiral the velocity of a step must be somewhat slower, i.e., the equation of the spiral must take into account the dependence of step velocity on distance from the center. However, in calculating the fundamental characteristics of the process it is sufficient to assume

$$\lambda = 4\pi\varrho_c.$$

Then the normal growth rate of a face, due to a single screw dislocation, is

$$V = \frac{a}{\lambda} v = \frac{\beta akTc_e}{4\alpha} \frac{\sigma^2}{1 + \frac{\beta a}{D} \ln \frac{\delta\sigma_c}{a\sigma} \operatorname{sh} \frac{\sigma}{\sigma_c}}, \quad (15.1)$$

where $\sigma_c = 4\Omega\alpha (kT\delta)^{-1}$. The product βa is the "diffusion" coefficient of crystal particles through the crystal-solution interface. $\beta a \sim D$ can be taken as a rough approximation, although a smaller value is actually possible because of entropy factors and because of the high activation energy of diffusion in a partially ordered layer of liquid directly in contact with the crystal.

For the purpose of obtaining a qualitative estimate we assume $\Omega = 3 \times 10^{-23}$ cm^3, $\alpha = 3 \times 10^2$ erg/cm^2, $kT = 5 \times 10^{-14}$ erg, $\delta = 7 \times 10^{-5}$ cm, $D = 10^{-5}$ cm^2/sec, $c_e = 10^{21}$ cm^{-3}, and obtain $\sigma_c = 10^{-2}$, $\frac{\beta akTc_e}{4\alpha} = 0.4$ cm/sec. A plot of $\frac{4\alpha V(\sigma)}{\beta akTc_e}$ for $\delta = 7 \times 10^{-5}$ cm ($\sigma_c = 10^{-2}$) and $\delta = 3.5 \times 10^{-5}$ cm ($\sigma_c = 2 \times 10^{-2}$) is shown in Fig. 15. At very low supersaturations $\sigma \ll \sigma_c$ we have $V \sim \sigma^2$. In this case spiral steps are widely separated, their concentration fields do not overlap ($\pi\delta \ll \lambda$), and they do not interfere with each other's supply of material. With increasing σ and closer spiral turns we have the almost linear relation

$$V = \frac{D\Omega c_e}{\delta} \sigma - \left(1 + \frac{\beta a}{D} \ln \frac{\sigma_c\delta}{2\sigma a}\right) \frac{D^2\Omega c_e\sigma_c}{\beta a\delta}. \quad (15.2)$$

This straight line passes below the coordinate origin and intersects the σ axis at $\sigma = \left(\frac{D}{\beta a} + \ln \frac{\delta\sigma_c}{2a\sigma}\right)\sigma_c.$

For $\sigma_c = 2 \times 10^{-2}$, $\delta = 3.5 \times 10^{-5}$ cm, i.e., curve 1 in Fig. 15, in the interval $0.01 < \sigma < 0.2$ the following approximation is accurate to within $\sim 3\%$:

$$V(\sigma) = \frac{\beta akTc_e}{4\alpha} M\sigma^m,$$

where M = 400 and m = 1.65. For different numerical values of σ_c and δ a similar approximation can be made, using somewhat different values of M and m.* The exponent m increases as σ_c increases or δ decreases; the region of the quadratic form of $V(\sigma)$ is enlarged as the solution is stirred more vigorously.
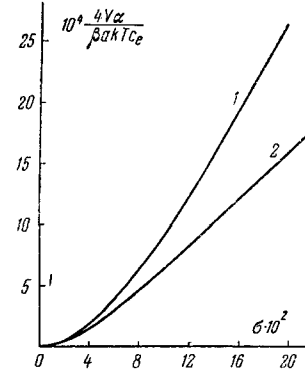

FIG. 15. Normal rate of dislocation growth from the solution as a function of supersaturation, assuming unit Burgers vector and no disintegration of the step with increasing supersaturation. Curve 1 — $\delta = 3.5 \times 10^{-5}$ cm; curve 2 — $\delta = 7 \times 10^{-5}$ cm.

In the assumed model the slope $\frac{dV}{d\sigma}$ depends on face orientation only in the nonlinear region. In the linear region the straight lines $V(\delta)$ for different faces (and identical δ) have identical slopes. This should not occur if particles adsorbed on crystal faces play an essential role in the growth process (Ch. II). Therefore experimental information concerning the anisotropy of dislocation-induced growth rates at different supersaturations could be important in studying the effect of self-adsorption and surface diffusion on the kinetics of growth from solution.

16. Some Experimental Results

Experimental determination of the growth rates of single crystals from solution has sometimes confirmed the existence of a linear region at low supersaturations. Examples of this are the old data of Marc[64] and of Wenk,[65] which, to be sure, were interpreted by them on the basis of ideas concerning bimolecular reactions. Similar evidence is found in the effect of supersaturation on crystal habits.

Kozlovskii[66] has measured directly the angular velocity of "rotation" of a spiral step on crystals of β-methyl naphthalene growing from an alcohol solution flowing over them. A computation based on Kozlov-

---

*In the interval $\sigma_1 < \sigma < \sigma_2$ we can determine M and m by using, for example, least-square deviation condition:

$$\int_{\sigma_1}^{\sigma_2} [V(\sigma) - M\sigma^m]^2 d\sigma = \min.$$

skii's data gives $V \sim \sigma^{1.83}$ for the normal growth rate of a spiral hill, in good agreement with the result given above.

A somewhat different nonlinear form of $V(\sigma)$ has been obtained by Dunning and Albon[67] for saccharose and by Follenius[68] for $NaClO_3$. The former investigators obtained a straight line not passing through the origin. Growth is entirely absent at supersaturations below a critical value. A similar critical point is described by Follenius, with subsequent increase of the growth rate showing a better than linear dependence on supersaturation.[68]

17. Growth from the Melt

It is difficult at the present time to furnish a unique description of the crystal-melt interface. This boundary can have a stepped structure, entirely analogous to that of the discussed crystal-vapor interface. On the other hand, in the case of some other crystals, face orientations, and temperatures, thermal fluctuations can apparently[14,69,70] disrupt close-packed faces, making them rough on an atomic scale. These faces will lack steps entirely, or, more accurately (reference 142, p. 304), will have them everywhere, i.e., kinks are uniformly distributed over the entire surface. The growth of these faces does not require nucleation, dislocations etc., and is limited only by thermal conduction and the relaxation times required for incorporating individual particles into the crystal lattice.

The appearance, during growth, of rounded surfaces that coincide with isotherms, favors the hypothesis of uniformly distributed kinks. Also, spiral growth from the melt has been observed directly on crystals of β-methyl naphthalene[66] and salol.[71] Stepped surfaces have been observed, following removal of the melt, by Graf,[72] Elbaum and Chalmers,[73] and Tiller[74] (for Zn, Cd, Au, Pb, Sn, and NaCl). In addition, some experiments (see the table) have revealed a nonlinear dependence of the normal growth rate on undercooling, which also indicates the possibility of layer growth at dislocations.

Substance	Experimental function $V(\Delta T)$	
Water[62]	$1,6 \cdot 10^{-1}$	$\Delta T^{1,7}$
Water[78] from $-2°$ to $-3.1°C$	$1,3 \cdot 10^{-2}$	$\Delta T^{2,9}$
from $-3°$ to $-6.5°C$	$7,55 \cdot 10^{-2}$	$\Delta T^{2,32}$
Glycerin[79]	$8 \cdot 10^{-6}$	$\Delta T^{1,7}$
Salol[80] $(\Delta T \leqslant 6°)$ . . .	$4 \cdot 10^{-4}$	$\Delta T^{1,7}$
Salol[80] $(\Delta T \geqslant 6°)$ . . .	$1,56 \cdot 10^{-5}$	$\Delta T^{2,3}$
Tin[81]	$7 \cdot 10^{-1}$	$\Delta T^{1,8}$
Phosphorus[82,83]	$1 \cdot 0$	$\Delta T^{1,7}$

We shall now consider the growth kinetics of surfaces that are not disturbed by thermal fluctuations. We shall first determine the rate of advance of a sequence of elementary steps. On the end-faces of steps, where crystallization takes place, the following condition, similar to (14.1), must be fulfilled:

$$\varkappa \frac{\partial T}{\partial r} = q\beta_T (T_0 - T), \quad r = a, \tag{17.1}$$

where $\varkappa$ is the coefficient of thermal conductivity, q is the latent heat of crystallization, and T_0 is the melting point. A step adjacent to the melt possesses a high density of kinks (higher, at least, than in a step adjacent to the vapor). Therefore the coefficient $\beta_{T'}$, which plays the same part as β in Ch. II and which characterizes the crystallization rate on a step, is derived in the simplest case from the general theory of the motion of a phase boundary possessing a large number of active sites:

$$\beta_T = \frac{Dq}{\Omega lkT_0^2}, \tag{17.2}$$

where $D \sim \nu l \exp\left(-\frac{\Delta U}{kT}\right)$ is the coefficient of diffusion through the potential barrier, of length l cm and height ΔU erg, near the end-face of a step. We note that an expression for β in Sec. 15 can be obtained similarly. Assume that the heat of crystallization is conducted away most intensely through the crystal. This is most typical, since the thermal conductivity of crystals is usually more than one order of magnitude greater than that of liquids.* Also, let the temperature gradient in the crystal be determined from the characteristic distance δ and $T(0,\delta) = T_\delta$. (The same coordinate system is used as in Sec. 14; for the case of the growth of a crystal platelet on a refrigerator, for example, δ is the platelet thickness.) For a rigorous solution, instead of introducing δ, the fine structure of the temperature field near the stepped surface must be considered as well as the macroscopic temperature distribution over the entire crystal.

The temperature distribution is determined by equations of the same type as for the concentration distribution considered in Sec. 14. Therefore (14.3) and (15.1) can be used immediately to write the following expressions for the rate of advance of a sequence of elementary steps and for the normal rate of spiral hill growth:

$$v = \pi\Omega\beta_T (T_0 - T) = \frac{\pi\Omega\beta_T (T_0 - T_\delta)}{1 + \frac{\beta_T qa}{\varkappa} \ln \frac{\lambda}{\pi a} \operatorname{sh} \frac{\pi}{\lambda} \delta},$$

$$V = \frac{a\beta_T qT_0}{4\alpha} \frac{\sigma^2}{1 + \frac{\beta_T qa}{\varkappa} \ln \frac{\delta\sigma_c}{a\sigma} \operatorname{sh} \frac{\sigma}{\sigma_c}}, \tag{17.3}$$

where $\sigma = \frac{T_0 - T_\delta}{T_0}$ and $\sigma_c = 4\Omega\alpha (q\delta)^{-1}$. When $\sigma \gg \sigma_c$, we can rewrite the second equation in (17.3) as

$$V = \frac{a\beta_T qT_0}{4\alpha} \frac{\sigma^2}{1 + \frac{a\beta_T q}{\varkappa\sigma_c} \sigma}. \tag{17.3a}$$

The formula of Hillig and Turnbull,[62] which assumes

---

*The conduction of heat of crystallization through a stirred melt (in the case of an isolated crystal in the melt) is entirely analogous to growth from the solution.

$\kappa = \infty$, can be obtained from (17.3), to within a factor of the order of unity, for $\dfrac{a\beta Tq}{\kappa} \to 0$. We then have $V \sim \sigma^2$. On the other hand, larger values of $\dfrac{a\beta Tq}{\kappa}$ result in the linearity of $V(\sigma)$. Therefore, to observe the quadratic range of $V(\sigma)$ we require high thermal conductivity κ and a small characteristic size δ.

We shall now estimate the order of magnitude of the coefficients in (17.2) and (17.3). Assuming, for water, $l \sim a = 3 \times 10^{-8}$ cm, $\Omega = 3 \times 10^{-23}$ cm^{-3}, $\alpha = 5$ erg/cm^2, q = 1.4 kcal/mole, $T_0 = 3 \times 10^2$ deg, $\kappa = 5 \times 10^{-2}$ cal/cm-sec-deg, D = 0.5×10^{-5} cm^2-sec, we obtain $\beta_T = 3 \times 10^{22}$ cm^{-2} sec^{-1} deg^{-1}, $\dfrac{a\beta Tq}{\kappa} = 4 \times 10^{-5}$, $\dfrac{a\beta TqT_0}{4\alpha} = 1.4 \times 10^3$ cm/sec, and $\sigma_c = 6 \times 10^{-9} \delta^{-1}$. Values of the same order are obtained for crystals with higher melting temperatures, such as tin.

As in the case of growth from solution, $\dfrac{4\alpha V(\sigma)}{a\beta TqT_0}$ can be approximated by $M\sigma^m$. M and m are determined from the values of the parameters in (17.3). For example, with accuracy $\sim 2 - 3\%$, in the interval $10^{-3} < \sigma < 16 \times 10^{-3}$, $\dfrac{4\alpha V(\sigma)}{a\beta TqT_0} = 0.275\,\sigma^{1.85}$ when $\dfrac{a\beta Tq}{\kappa\sigma_c} = 3 \times 10^2$ (for the numerical values given above this corresponds to $\delta \cong 5 \times 10^{-2}$ cm), while the result is $0.085\,\sigma^{1.71}$ or $0.0275\,\sigma^{1.6}$ for $\dfrac{a\beta Tq}{\kappa\sigma_c} = 6 \times 10^2$ ($\delta \cong 10^{-1}$ cm) or $\dfrac{a\beta Tq}{\kappa\sigma_c} = 12 \times 10^2$ ($\delta \cong 2 \times 10^{-1}$ cm), respectively. These estimates indicate a relatively slight dependence of $\dfrac{a\beta Tq}{\kappa\sigma_c} = \dfrac{a\beta Tq^2\delta}{4\Omega\alpha\kappa}$ on the exponent m, but strong dependence on M.

The dependence of the growth rate on undercooling agrees satisfactorily with some of the data in the table. The discrepancies for water and salol (m > 2) can be associated with the large degrees of undercooling to which these experimental data pertain, and with growth due to nucleation. An exponent of σ greater than 2 has also been observed in dislocation growth from vapor[23] (Sec. 11); the similar value in growth from the melt can result from the same cause.

The foregoing calculations have ignored completely the probability that two-dimensional nuclei appear on the crystal surface, although this probability can be large in virtue of the low surface energy at the crystal-melt interface. Hillig[77] has obtained experimentally the dependence of the growth rate of ice on undercooling, due to the formation of two-dimensional nuclei.

A value of M agreeing in order of magnitude with experimental results has been obtained for glycerin and salol. In (17.2) D, the diffusion coefficient through the boundary potential barrier, was assumed to equal the self-diffusion coefficient in the melt and was found from viscosity data. This assumption, in the opinion of the authors, can account for the fact that the values of M calculated for water, tin, and phosphorus are one to three orders of magnitude lower than the experimental values. A more important cause evidently lies in the imperfect surfaces of rapidly growing Pb, Sn, and H_2O.

18. The Diffusion Field and Rate of Advance of a Macroscopic Step

In order to determine the rate of advance and shape of a macroscopic step in growth from solution, one must first determine the concentration distribution of the solution above the step. This has been done by Seeger in a stationary approximation to within additive and multiplicative constants.[84] He found that the concentration c(x,y) satisfies Laplace's equation $\Delta c = 0$, and that the profile of a macroscopic step is as depicted in Fig. 16. The front BC is a sink for dissolved particles, with the current $D\dfrac{\partial c}{\partial y} = j = $ const. On the other surfaces we have $\dfrac{\partial c}{\partial n} = 0$. When the upper left-hand region of the complex plane z = x + iy is mapped conformally on the upper half of the plane $\zeta = \xi + i\eta$ with the aid of the Schwarz-Christoffel integral

$$z = \frac{h}{2\varphi_0} \int_0^\zeta \left(\frac{1+t}{1-t}\right)^{\varphi_0/\pi} dt,$$

we obtain

$$c(\xi,\eta) = \frac{jh}{2\pi\varphi_0 D} \int_{-1}^{+1} \left(\frac{1+u}{1-u}\right)^{\frac{\varphi_0}{\pi}} \ln\sqrt{(\xi-u)^2 + \eta^2}\,du + R. \quad (18.1)$$

The unknown constants R and j, the latter of which is proportional to the rate of advance of the step, are easily obtained for a sequence of parallel macroscopic steps separated by $\lambda \gg 2s_0 = 2h\sin\varphi_0$. For $\delta > \sqrt{x^2 + y^2} > s_0$ the diffusion field of each step coincides with the field of a line source of strength $2js_0$, and $c(0,\delta) = c_\delta$. This concentration distribution is given by (18.1). When corresponding coefficients are equated, we have

$$R = c_\delta - \frac{2js_0}{\pi D}\ln\frac{2\varphi_0\lambda}{\pi h}\,\text{sh}\,\frac{\pi}{\lambda}\delta. \quad (18.2)$$

For steady-state advance of steps at low supersaturation,

$$j = \beta(c(x,0) - c_e) = \frac{V}{\Omega}\sin\varphi_0. \quad (18.3)$$

The equilibrium concentration of the solution (Sec. 2) is

$$c_e = c_{e0} + \frac{c_{e0}\Omega}{kT}\frac{\partial^2 F}{\partial P^2}\bigg|_{P=P_0=\text{tg}\,\varphi_0}\frac{dp}{dx} \equiv c_{e0} + E\frac{d\xi}{dx}\frac{dp}{d\xi}. \quad (18.4)$$

Equations (18.3), (18.4), and (18.1) determine a first-order differential equation for p(ξ). The two boundary conditions p($\pm$1) = p_0 furnish the integration constant and V_t. The departure of the profile of BC (represented by the dashed line in Fig. 16) from a straight line is thus calculated to be proportional to
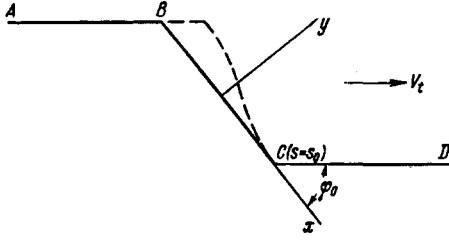
FIG. 16. Profile of a macroscopic step. The dashed line represents the profile change of a non-close-packed end face in growth from solution.

σ. A small correction $\sim \sigma^2$ takes account of the corresponding distortion of the diffusion field* of the step. Thus

$$p(\xi) = p_0 + \frac{jh^2}{4\pi\varphi_0^2 DE}\int_{-1}^{\xi}\int_{-1}^{+1}\left(\frac{1+w}{1-w}\right)^{\frac{\varphi_0}{\pi}}\left(\frac{1+u}{1-u}\right)^{\frac{\varphi_0}{\pi}}\ln|w-u|\,du\,dw$$

$$+ \frac{h}{2\varphi_0 E}\left[(c_\delta - c_e) - \frac{j}{\beta} - \frac{2js_0}{\pi D}\ln\frac{2\varphi_0\lambda}{\pi h}\,\text{sh}\,\frac{\pi}{\lambda}\,\delta\right]\int_{-1}^{\xi}\left(\frac{1+u}{1-u}\right)^{\frac{\varphi_0}{\pi}}du.$$

$$\text{(18.5)}$$

The rate of advance of a step (in the sequence) is

$$V_t = f(h,\ \delta,\ \lambda)\,\Omega\beta\,(c_\delta - c_e),$$

where

$$f(h,\ \delta,\ \lambda) = \frac{\sec\varphi_0}{1 + \dfrac{\beta h}{\pi D\sin\varphi_0}\ln\dfrac{2\varphi_0\lambda}{\pi h}\,\text{sh}\,\dfrac{\pi}{\lambda}\,\delta + \dfrac{\beta h\sin\varphi_0}{4\pi\varphi_0^2 D}K(\varphi_0)},$$

$$K(\varphi_0) = \int_{-1}^{1}\int_{-1}^{1}\left(\frac{1+w}{1-w}\right)^{\frac{\varphi_0}{\pi}}\left(\frac{1+u}{1-u}\right)^{\frac{\varphi_0}{\pi}}\ln|w-u|\,du\,dw. \quad \text{(18.6)}$$

Surface energy enters the expression for V_t only through the angle φ_0, so that V_t is independent of its absolute value. When $\beta a \sim D$ the second, third, and fourth terms in the denominator of f are, as a rule, considerably larger than unity. Therefore, in accordance with (14.3) the rate of advance of a step decreases with height as $\sim 1/h$.

The shape of a non-close-packed end face is described by the complicated function (18.5). Simplifying the problem and assuming a linear increase of concentration of the solution from B to C, we find, by the same procedure as for (18.5) and (18.6), that at low supersaturations $\varphi(s)$ is the parabola 3 in Fig. 10.

The corresponding step profile is represented schematically by the dashed line in Fig. 16. If the condition (10.8) for the stability of a macrostep, which condition is associated with the surface energy is violated for $p = p_0 + p_c$, then all steps for which

$$h > \text{const} + [(p_c - p_0)\sigma]^{-1/2},$$

must break down.

It is clear from Fig. 16 that breakdown should result in the formation of a layer overhanging the sur-

*Temkin[99] and others have considered the way in which the stability of a flat surface is affected by the temperature redistribution that accompanies a random change of shape.

face, rather than in the formation of a lower macroscopic step as in growth from vapor (Sec. 10). This results directly from neglect of the stream of particles adsorbed on the surface and from feeding of the end face only through volume diffusion, which obviously insures a higher concentration of the solution around the salient corner B than near the reentrant corner C (Fig. 16). This distribution not only fails to generate macrosteps, but also supports the stability of the original step against not too great variations of its shape that maintain the basic character of the $\varphi(s)$ curve. In the assumed model, decay resulting in the emission of lower steps can occur, either through nucleation in the reentrant corner C (Sec. 10) or for some other kinetic reasons.

IV. THE INTERACTION OF GROWING CRYSTALS WITH IMPURITIES

The interaction of growing crystals with impurities is known to bring about several effects — change of the growth rate, impurity capture, crystal defect formation (internal strains, dislocations, micro- and macro-inclusions, etc.). Some of these effects are discussed in the present section. Our entire treatment will, as heretofore, be based on the layer growth of crystals resulting from the motion of steps.

We shall first consider two of the possible mechanisms of slowed crystal growth due to impurities during layer growth from different phases. We shall then study the conditions for equilibrium and non-equilibrium impurity capture, and shall calculate the coefficient of non-equilibrium impurity capture depending on the growth rate and the orientation of the growing face (the sector structure of crystals[85]) and on the height of the steps whose advance produces growth. At a given growth rate, the greater the average step height, the more the capture coefficient departs from its equilibrium value.

19. The Influence of Impurities on the Growth Rate

An impurity usually lowers the growth rate. The strongest effect is produced by organic substances with large molecules.[86,87] A considerable reduction of the growth rate is observed even when only one such molecule is present in $10^4 - 10^6$ molecules of the solution. An important characteristic of this kind of impurity is its inability (at least at low concentrations) to influence appreciably the dissolution rate of crystals. Certain inorganic ions are also effective in very small quantities. For example, Fe^{3+} at molar concentrations $\sim 10^{-6}$ reduces by about one order of magnitude both the growth rate and the dissolution rate of LiF crystals.[88] Also, the addition of $\sim 0.02\%$ Na_2SO_4 to the solution lowers the growth rate of octahedral faces of $NaClO_3$ crystals to one-fourth, and halves the growth rate of cubic faces.[89]

The few experiments in which the growth rate in-

creased[90,91] are accounted for either by the catalytic effect of an impurity,[90,91] or by lowered surface energy, smaller size of the critical nucleus, and enhanced probability of nucleation.[92-94]

Impurities lower the growth rate primarily as a result of their adsorption on surfaces and at active growth sites. The theory of impurity adsorption at crystallographically different surface positions, of the influence of adsorption on surface energy, and of nucleation probability was developed and is continuing to be developed by the Stranski-Kaischew school.[4-9,92,93,95,96] We shall discuss the fundamental kinetic effects, without considering the energy aspects in detail.

a) Strongly adsorbed impurities captured by a growing crystal.[87] Let some large (organic) crystals be adsorbed strongly on a crystal surface. During the growth process steps are retarded at the points of contact with these molecules and are therefore forced to "filter through" the "palisade" of surface impurities. All of these impurity particles are captured by advancing steps, and are replaced with new impurity molecules passing from the parent liquid to the newly deposited layers. If ρ_c is the radius of curvature of a critical nucleus, a is the step height, and J_i is the impurity current to the growing surface, then growth in the presence of impurities takes place only at supersaturations where the normal growth rate without impurities is

$$V > 14 a \rho_c^2 J_i.$$

In other words, when $\rho_c \sim \sigma^{-1}$ and $V \sim \sigma^m$ growth in the presence of impurities takes place only at supersaturations

$$\sigma > \sigma^* = \mathrm{const} \cdot J_i^{\frac{1}{2+m}}. \qquad (19.1)$$

At the critical supersaturation given by (19.1) the diameter of the critical nucleus equals or exceeds the mean distance between adsorbed particles, between which the step cannot "filter through" in this case.

The discussed model of Cabrera and Vermilyea[87] should also furnish correct results for the growth rate in a porous medium (such as a gel) when the characteristic pore size is comparable with the critical diameter of nuclei.

An impurity slows the advance of elementary steps whose height is comparable to that of the adsorbed impurity molecules; this effect is reduced as step height increases. The influence of impurities on the normal growth rate must therefore depend particularly on the mean step height.

Equation (19.1) is applicable when the relaxation time τ required to establish an equilibrium concentration of impurities on the surface is small compared with the time h/V that elapses between the deposition of successive layers. Therefore, when $V \sim 10^{-3} - 10^{-4}$ cm/sec and $h \sim 10^{-7}$ cm, if $\tau \gtrsim 10^{-3} - 10^{-4}$ sec the

dependence of J_i on the growth rate of a face must be taken into account.[56]

b) Impurity poisoning of kinks. When adsorbed impurities have a short lifetime on the surface, the described mechanism cannot play an essential role, but is replaced in importance by impurity poisoning of active growth sites (kinks). Impurity adsorption on a surface and step, and in kinks, is represented schematically in Fig. 17 (positions 5, 2, and 3). When an impurity is only poorly captured by a growing crystal, it is practically impossible to incorporate new particles into the crystal in poisoned kinks. Assuming that the kinks are uniformly distributed on the surface and that the growth rate V is proportional to the number of active sites free of impurities, Bliznakow[96] derived the dependence of V on impurity concentration c_i in the form

$$V(c_i) = V(0) - [V(0) - V(\infty)] \frac{c_i}{c_i + B}, \qquad (19.2)$$

where $\dfrac{c_i}{c_i + B}$ represents the fraction of active sites occupied by impurities (Langmuir's adsorption isotherm).

Kinks are actually concentrated in steps instead of being uniformly distributed on the surface. With respect to the diffusion of crystallizing material, the actual kink distribution is qualitatively equivalent to a uniform distribution only when the distance λ between steps is much smaller than the characteristic diffusion parameters (λ_s in Ch. II and δ in Ch. III), or when the distance between impurity-free kinks is $\lambda_0(c_i) > \lambda$. The first of the given conditions is fulfilled for growth at dislocations or at high supersaturations with a linear form of $V(\sigma)$, while the second condition is fulfilled at very high impurity concentrations. The kink distribution in steps will be used below.[97]

The density λ_0^{-1} of kinks unoccupied by impurities is easily derived in the same manner as the kink density in a pure step (Ch. II, Sec. 6). For a crystal in contact with an ideal gas impurity

$$\lambda_0(P_i) = \frac{a}{2} \left\{ 2 + \exp\left(\frac{w_1}{kT}\right) \middle| + \frac{P_i(kT)^{1/2}}{(2\pi m)^{3/2} \nu^3} \left(\exp \frac{w_g + w_1 - w_3}{kT} \right.\right.$$
$$\left.\left. + \exp \frac{w_g + w_1 - w_g}{kT} \right) \right\} \equiv \lambda_0(0) + \xi_g P_i, \qquad (19.3)$$

where P_i is the partial gas pressure of the impurity, m is the mass of an impurity particle, ν ($\sim 10^{12}$ sec^{-1}) is its vibrational frequency in the adsorbed state, w_g is the particle energy in the gaseous phase, w_2 is its energy in the adsorbed position at the step (position 2, Fig. 17), w_1 is the energy of a free kink, and w_3 is the energy of an impurity-occupied kink. When the adsorption energy in a kink is $w_g + w_1 - w_3 = 0.5$ ev (~ 12 kcal/mole), $T = 300°$K, and $m = 50 \times 1.6 \times 10^{-24}$g, then $\xi_g = 10^{-2}$ a/bar. Consequently, at impurity pressures of the order of 1 mm Hg most kinks should be poisoned.
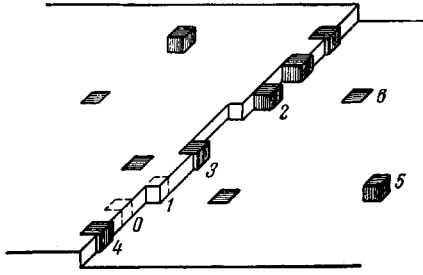
In the case of an ideal solution of an impurity with

FIG. 17. Impurity particles (the dark blocks) on a crystal sur-
face: 2 — adsorbed on a step, 3 — in a kink, 5 — on the surface,
4 — in a step, 6 — in the surface layer. 0 and 1 are crystal particles.

FIG. 18. The normal
rate of dislocation-induced
growth as a function of im-
purity gas pressure.

concentration c_i surrounding the crystal, we obtain,
similarly,

$$\lambda_0(c_i) = \lambda_0(0) + \xi_s c_i. \qquad (19.4)$$

Here $\xi_S = \dfrac{a}{2\Omega\nu^3}\left(\dfrac{kT}{2\pi m}\right)^{3/2} \exp\dfrac{w_S + w_1 - w_3}{kT}$, Ω is
the molecular volume of the solution, w_S is the energy
of an impurity particle in the solution, and ν is its
vibrational frequency in the adsorbed state. When, for
the purpose of an estimate, we take $w_S + w_1 - w_3 \sim 0.4$
ev (~ 10 kcal/mole) and $\nu \sim 3 \times 10^{12}$ sec, we obtain
$\xi_S \sim 10^4 a$, i.e., an impurity concentration $\sim 10^{-3}$ is
sufficient for greatly increased distances between near-
est free kinks. The expressions given for the constants
ξ_g and ξ_S are approximate, but their magnitudes are
very strongly dependent on the adsorption energy, tem-
perature, vibrational frequency, and mass of an im-
purity particle. The given estimates are thus of a
provisional nature, and only indicate the theoretical
possibility of the step-poisoning effect.

We shall now explain the way in which the tangential
and normal growth rates from the vapor depend on im-
purity concentration. This dependence obviously enters
through the coefficient β, which at low kink density can
be assumed to have the form*

$$\beta = \frac{\beta_1}{\lambda_0}. \qquad (19.5)$$

Substituting in (7.9) and (9.2) and using (19.3) for λ_0,
we obtain the tangential and normal growth rates as
functions of the impurity partial gas pressure, which
is plotted in Fig. 18 for $\dfrac{2\lambda_S}{\beta\tau_S} = \dfrac{2\lambda_S\lambda_0(0)}{a^2\tau_S} = 1$, i.e.,

$\lambda_0(0) = 4a$, $\dfrac{W}{kT} = 24$, $\nu\tau = 50$ [τ is the relaxation

time (Sec. 7)], and $\xi_g = 10^{-2}$ a/bar. If it is assumed
that even a completely poisoned step can grow,[96,94]
then as $P_i \to \infty$ the rate V should approach a finite
limit, as in (19.2) when $c_i \to \infty$. The relationship
(19.2), which is close to that represented in Fig. 18,
was observed by Bliznakow[96] for growth from solution.
When β is reduced, an impurity should not only slow
the normal growth rate V, but also extend the non-

*Reference 14 contains a detailed calculation of $v(\lambda_0)$. How-
ever, the incorrect step boundary condition (7.5) used there makes
the result only qualitatively correct.
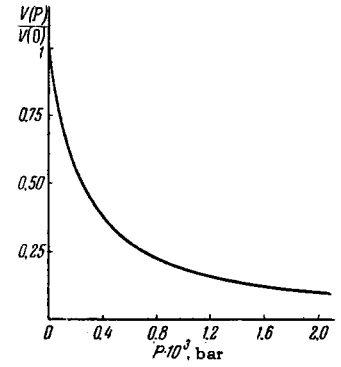
linear region of $V(\sigma)$. This effect is illustrated in
Fig. 8, where curve 2, which was plotted for smaller
β, can be regarded as representing the function $V(\sigma)$
in the presence of impurities.

The impurity adsorption energy on a step is gener-
ally dependent on step orientation. Therefore we can
expect that in the presence of an impurity the aniso-
tropy of $\lambda_0(P_i)$ will be accompanied by anisotropy of
the rate of step advance, manifested by a noncircular
step shape and, specifically, in the polygonization of
steps. The impurity effect should depend on tempera-
ture [see (19.3)].

Impurity adsorption in a step lowers the surface
energy α of the end-face and therefore, according to
(9.2), (15.1), and (17.3), should tend to enhance the
growth rate at a dislocation.[94,96] The diminishing of
α increases both the probability of nucleation and the
growth rate of a perfect face. The latter effect has
been observed experimentally by Sears.[94]

An impurity that is adsorbed at kinks of a step in
contact with the solution reduces β according to (19.5)
and (19.4). Therefore the character of the dependence
of the normal growth rate from solution on impurity
concentration, as well as the impurity effect on the
form of $V(\sigma)$ will be the same as in growth from the
gaseous phase. A moving step rejects an impurity and
becomes its line source. In the case of very slow
crystal growth, the impurity concentration c_i near a
step can be identified with its mean concentration in
the solution. When the growth rate exceeds the im-
purity diffusion rate in the solution, the concentration
near steps exceeds the volumetric concentration. The
diffusion field of impurities above a sequence of ele-
mentary and macroscopic steps can in the simplest
cases be calculated as in Secs. 14 — 15.

Kinks in a step are poisoned by impurities in both
growing and evaporating (or dissolving) crystals.
Therefore the formulas used in growth can describe
the effect that impurities of the considered type have
on the evaporation rate.

In the steady-state advance of a macroscopic step
the concentration of impurity repelled by the crystal
near the reentrant corner CC' (Fig. 9) is higher than
near BB'. If the impurity slows growth, this distribu-
tion should obviously promote macrostep stability. In
growth from the melt an impurity distributed in the

described manner drops the melting point lower in the better cooled region around CC' and less in the better heated region near BB'; breakdown of the macrostep is thus prevented.[75] The method of conformal representation used above will perhaps furnish a solution of the still unsolved problem of obtaining jointly the impurity concentration and temperature near a macrostep.

20. Nonequilibrium Capture of Impurities in Crystal Growth

When the system consisting of a crystal and the surrounding medium contains an impurity, the impurity concentration c_C in the crystal and c_L in the medium under conditions of equilibrium are related to the phase diagram. The ratio $c_C/c_L = k_0$ is called the (equilibrium) coefficient of distribution (or capture). If the crystal grows very slowly, its impurity concentration is determined by the equilibrium capture coefficient and by c_L^* in the medium at the interface. When $k_0 < 1$ (the crystal rejects the impurity), c_L^* will increase with the growth rate. Therefore the equilibrium capture coefficient increases effectively with the growth rate. Rigorous calculations of the impurity concentration in the surrounding medium, of the macroscopic temperature distribution, and of the associated effects for different cases are to be found in papers by Lyubov and his co-workers,[98,99] by Ivantsov,[100,101] and by Tiller, Chalmers and others.[102-104] Without pausing to consider the results obtained in this important direction of phenomenological investigation, we shall concentrate our attention on the elementary processes of nonequilibrium impurity capture.[105]*

The equilibrium impurity concentration is not constant throughout the crystal, since a difference exists between its value near the surface and in the bulk. The equilibrium concentration can be characterized approximately by three quantities — the concentrations c_V in the bulk crystal, c_S in the surface layer (position 6, Fig. 17), and c_E in steps (position 4, Fig. 17). These quantities, which are determined by the heats of solution and entropies of the three-, two-, and one-dimensional "solid solutions," can differ considerably from each other (by a factor of several units).[105] c_S and c_E depend on the crystallographic orientation of the surface and step.

Different relaxation times are also required to establish equilibrium in the three "phases" (three-dimensional, two-dimensional and one-dimensional). A (three-dimensional) volume possesses the longest relaxation time, while the shortest time is associated with the one-dimensional case (relaxation by means of diffusion in the crystal).

*"Elementary processes" are microscopic phenomena in the macroscopic interfacial layer whose thickness is of the order of the characteristic size of a surface inhomogeneity, such as the distance between steps, a step height etc.

If the crystal grows very slowly, an equilibrium impurity concentration exists in all three "phases." At high growth rates equilibrium is not established in the bulk, but in the surface layer and steps, or only in the steps. However, each surface layer soon becomes an interior layer with an equilibrium impurity concentration. This also applies to the line or band of atoms forming the end face of a step. At still higher growth rates none of the three equilibrium concentrations (c_V, c_S, and c_E) is achieved. Therefore when new layers are deposited on the crystal surface (as a result of advancing steps, for example) the impurity concentration in these layers will not generally be in equilibrium, and impurity diffusion from or to the crystal will begin. If the thickness of a newly deposited layer is denoted by h, and the impurity diffusion coefficient in the crystal by D_i, the diffusion rate is of the order D_i/h. If D_i/h exceeds appreciably the normal crystal growth rate V, impurity capture can reach equilibrium, but if $D_i/h \lesssim V$, then the crystal will have a nonequilibrium impurity content.

For germanium at $\sim 900°C$ the impurity diffusion coefficient of group-III and group-V elements is $10^{-9} - 10^{-12}$ cm^2/sec. Consequently, for $h \sim 10^{-7} - 10^{-6}$ cm we have $D_i/h \sim 10^{-2} - 10^{-6}$ cm/sec, i.e., even at such relatively high temperatures the capture of impurities cannot be regarded as in equilibrium when $V \gtrsim 10^{-4} - 10^{-5}$ cm/sec. The diffusion coefficient falls off exponentially with temperature. Therefore equilibrium impurity capture certainly does not exist at lower temperatures and the ordinary growth rates (such as growth from the solution at $V \sim 10^{-5} - 10^{-6}$ cm/sec). As an example of nonequilibrium impurity capture one must, of course, mention the sectoral structure of crystals (the "hourglass figures") that have been well-known for a long time.[85,139] Nonequilibrium impurity capture by germanium and silicon crystals growing from the melt were evidently observed in 1953 by Hall,[106] who established the dependence of the capture coefficient on growth rate and on face indices. The latter of these dependences is hardly amenable to interpretation if we confine ourselves to the consideration of diffusion in the liquid phase.

We shall now determine the nonequilibrium capture coefficient when diffusion in the solid phase is important ($D_i/h \sim V$). We shall assume that crystal growth involves the successive deposition on the surface, at equal time intervals, of identically thick layers, and that the velocity of advance of the step terminating each layer is infinite compared with the diffusion rate. The coefficient of impurity capture by steps is given. Let $c(x,t)$ be the impurity concentration in the crystal, $c_0(x)$ its equilibrium value, c_1 the initial concentration in a new layer, and $u(x,t) = c(x,t) - c_0(x)$. Then in the time interval between the depositions of successive layers, i.e., $0 < t < \tau_h = h/V$, the impurity

distribution in the crystal is described by the solution of the following boundary problem:

$$\frac{\partial u}{\partial t} = D_i \frac{\partial^2 u}{\partial x^2},$$

$$b \frac{\partial u}{\partial x} = u,$$

$$u(x, 0) = \begin{cases} c_1 - c_0(x), & 0 < x < h, \\ u(x-h, \tau_h) + c_0(x-h) - c_0(x), & x > h. \end{cases} \quad (20.1)$$

If D_i^* is the coefficient of impurity diffusion through the phase boundary of width $\sim a$, then we have the length $b \sim \frac{D_i}{D_i^*} a < a$, since diffusion through the interface is easier than diffusion in the bulk of the solid phase, and $D_i^* > D_i$.

As an approximation to the true equilibrium impurity distribution in the crystal we take the function

$$c_0(x) = \begin{cases} c_S & 0 < x < l, \\ c_V & x > l, \end{cases}$$

where l is the thickness of the surface layer in which the equilibrium impurity concentration c_S differs from the bulk equilibrium concentration c_V; l is of the order of magnitude of the interatomic spacing. We also assume that at the instant when each new layer is deposited the constant value $u(x, \tau) = u_C$ is established. Then (Fig. 19)
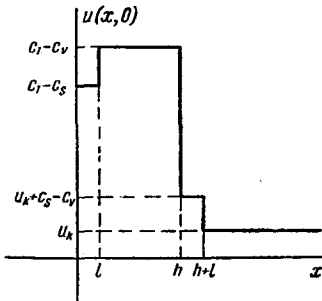

FIG. 19. Impurity distribution near a crystal surface immediately after the deposition of a new layer of thickness h. l is the thickness of the surface layer where the equilibrium impurity concentration differs from its value in the bulk crystal.

$$u(x, 0) = \begin{cases} c_1 - c_S & 0 < x < l, \\ c_1 - c_V & l < x < h, \\ u_C + c_S - c_V & h < x < h+l, \\ u_C & x > h+l. \end{cases} \quad (20.2)$$

We proceed as follows for the purpose of determining the unknown constant u_C. When a new layer of thickness h is deposited, impurities enter the crystal in the amount $c_1 h$. During the time τ_h impurities leave the crystal in the amount $-D_i \int_0^{\tau_h} \frac{\partial u}{\partial x}\Big|_{x=0} dt$.

On the other hand, from the definition of u_C the change of impurity content within the time from $t = 0$ to $t = \tau_h$ is

$$\int_0^\infty [u_C + c_0(x)]\, dx - \int_h^\infty [u_C + c_0(x-h)]\, dx = (u_C + c_V)\, h.$$

Therefore,

$$c_1 h - D_i \int_0^{\tau_h} \frac{\partial u}{\partial x}\Big|_{x=0} dt = (u_C + c_V)\, h.$$

u_C is obtained by substituting $u(x, t)$ derived from (20.1) — (20.2). The impurity capture coefficient k is then determined as the ratio of the mean impurity concentration in the crystal, $u_C + c_V$, to the impurity concentration c_L in the liquid at the interface. Introducing the notation $k = \frac{c_S}{c_L}$ and $k_1 = \frac{c_1}{c_L}$, we obtain the following expression for the capture coefficient:

$$k = \frac{g(l)+g(h)-g(h+l)}{h+g(h)} k_0 + \frac{g(0)+g(h+l)-g(l)}{h+g(h)} k_S$$

$$+ \frac{h-g(0)-g(h)}{h+g(h)} k_1, \quad (20.3)$$

where

$$g(\Delta) = b \exp\left(-\frac{\Delta^2}{4D_i\tau_h}\right) \exp\left(\frac{\Delta}{2\sqrt{D_i\tau_h}} + b^{-1}\sqrt{D_i\tau_h}\right)$$

$$\times \operatorname{erf} c\left(\frac{\Delta}{\sqrt{2D_i\tau_h}} - b^{-1}\sqrt{D_i\tau_h}\right) - (\Delta + b)\operatorname{erf} c\left(\frac{\Delta}{2\sqrt{D_i\tau_h}}\right)$$

$$+ 2\sqrt{\frac{D_i\tau_h}{\pi}} \exp\left(-\frac{\Delta^2}{4D_i\tau_h}\right)$$

Equation (20.3) can be simplified in the two limiting cases of large and small normal growth rate $V = h/\tau_h$, as follows:

$$k = k_0 + (k_S - k_0)\frac{lV}{4D_i} + (k_1 - k_0)(h + 2b)\frac{V}{4D_i}$$

$$\text{for} \quad V \ll \frac{D_i}{h},$$

$$k = k_1 + k_0 \frac{l}{h} - (k_1 - k_S)\frac{D_i}{bV}$$

$$\text{for} \quad V \gg \frac{D_i}{h}. \quad (20.3a)$$

Equation (20.3) is meaningful only for degrees of undercooling and step heights where the tangential rate of step advance obeys $V_t \gg D_i/h$. With $V_t \gg V$, Eq. (20.3) has a broad range of applicability.

The coefficient k_1 in (20.3) is not constant and can in turn depend on the growth rate according to (20.3). Indeed, if a high step can be represented as a cluster of parallel elementary monatomic steps, the calculation of k_1 becomes the foregoing problem with h replaced by the elementary step height a and with k_1 replaced by the coefficient of impurity capture by this step. Therefore at low growth rates the third term in (20.3) is actually quadratic in V and the entire function will be represented by Fig. 20.

The capture coefficient is dependent on the crystallographic orientation of the face primarily through k_1 and k_S. The parameter b and the diffusion coefficient D_i in (20.1) also depend on the indices of the growing surface.

Equation (20.3) furnishes evidence that the impurity capture coefficient depends on the stepped structure
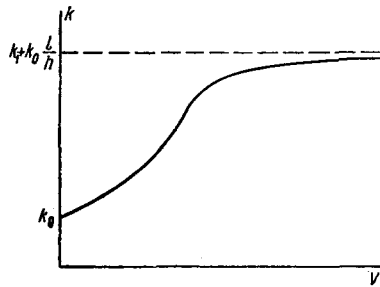
FIG. 20. The coefficient of nonequilibrium impurity capture as a function of the normal rate of layer growth.

of the surface (on the magnitude of h). Consequently, the factors that affect this structure (surface energy, supersaturation or undercooling, temperature, impurities etc.) can change the capture coefficient. We have so far assumed that a surface is formed of identical equidistant steps. The actual structure of a face is, of course, more complicated, being represented by the distribution $\rho(h, \lambda)$, where λ is the distance between steps (Sec. 10). When $\rho(h, \lambda)$ is found the true capture coefficient is expressed by the integral $\iint k(h, \lambda) \rho(h, \lambda) dh d\lambda$. A more detailed investigation should also take into account the nonuniform impurity distribution on the fronts of high steps (Sec. 18), their finite advance rate, and several other factors.

21. Dislocation Production in Impurity Capture

Impurity atoms (or molecules) captured by a growing crystal differ in size from the crystal constituents and therefore induce tensile strains in the lattice. A nonuniformly distributed impurity is associated with a nonuniform strained state. Large strains can be resolved by dislocations. Tiller[75] has suggested a specific mechanism. Consider a crystal growing from the melt by the deposition of macroscopically thick surface layers. In view of the nonuniform impurity distribution on the step front (from BB' to CC'), the impurity concentration in a thin crystal layer of thickness Δ remaining behind the CC' edge will be greater than in other parts of the layer deposited during step movement. If the radius r_s of impurity atoms exceeds that of crystal particles by Δr, then the Δ layer induces tensile strains in the remainder of the crystal; these are resolved by the dislocation grid shown in Fig. 9. If the crystallization isotherm is parallel to the mean surface of the crystal, making the angle θ with the orientation of the close-packed face, and if the lattice deformation is proportional to the impurity concentration, the dislocation density is

$$\varrho_g(\theta) = \frac{4k |\nabla T \Delta r| \cos\theta}{m r_s^2},$$

where $m = \left(\dfrac{\partial T_{melt}}{\partial c_i}\right)_p$ is the lowering of the crystal melting point due to an impurity concentration c_i. This analysis does not conflict with experiment.

Cabrera and Vermilyea[87] have discussed dislocation formation during the growth of a region with large local impurity content.

Kozlovskiĭ[107] has described the production of screw dislocations when macroscopic (1 − 10 micron) graphite particles were overgrown with lamellar crystals of β-methyl naphthalene. The mechanism involved here is very similar to that of dislocation production in the reentrant corner of a dendritic crystal (without impurities), as observed by Lemmleĭn and Dukova[108] and by Kozlovskiĭ.[107] Dislocation production in pure crystals has also been discussed in references 109 − 116.

V. ETCHING

Etching is known to represent either the simple dissolution or evaporation of a crystal (such as thermal etching in a vacuum), or its dissolution in a chemical reaction. In both instances elementary etching processes, like decrystallization generally, must run counter to the processes of crystal layer growth (Sec. 12). It is very important to note that etching sometimes takes place at very large undersaturations, whereas the above-discussed theory of growth and decrystallization pertains to small deviations from equilibrium. Nevertheless, the theory has qualitative application to this case also.

Regel', Urusovskaya, and Kolomiĭchuk[117] have published a review of work on the etching of dislocations, including an extensive bibliography of 264 titles and tables of etchants for different crystals. We shall here discuss briefly only the fundamental aspects of elementary processes of selective etching.

Let us consider a close-packed crystal face in contact with an etchant. Dissolution of the crystal sets in since the chemical potential μ of the crystal substance in the etchant is lower than the chemical potential μ_C of the crystal. Dissolution takes place by step movement in the direction opposite to that for growth. The sources of steps will again be screw dislocations, two-dimensional nuclei of dissolution (hollows of monatomic thickness in the surface layer of the lattice), subgrain boundaries, and the crystal edge. The probability of nucleation is greater on surface regions where the lattice energy density and the chemical potential are higher. These favored regions include the vicinity of points of emergence of dislocations, especially edge dislocations, as well as the sites of point defects. Therefore nuclei appear at dislocations more frequently than elsewhere, and etch pyramids are formed in these areas.[88] The shape of a pyramid depends on the ratio of the normal dissolution rate V, determined by the nucleation rate, to the tangential velocity V_t of the steps that originate at this time. For low values of V/V_t the pits are shallow, but become deeper and more easily observable as V/V_t increases. Therefore the addition of an impurity that

slows step motion but has a relatively slight effect on the probability of nucleation improves the quality of the pits. Impurities that increase V should have a similar effect. If a dislocation leaves its position we have V = 0; the pit acquires a flat bottom and then disappears entirely, as in the etching of point defects.

We have $V \sim \exp\left(-\dfrac{\Delta\Phi_C}{kT}\right)$, where $\Delta\Phi_C$ is the change in the thermodynamic potential of the system required for the production of a single dissolution nucleus of critical size ρ_C. When a dissolution nucleus with radius r is created the thermodynamic potential changes by the amount

$$\Delta\Phi(r) = -\frac{\pi r^2 a\,(\mu_C-\mu)}{\Omega} + \pi r a\alpha - \frac{a}{2}\int_0^r \frac{Gb^2}{r}\,dr,$$

Here G is the shear modulus and $\dfrac{Gb^2}{4\pi r^2}$ is the strain energy density near the dislocation. Figure 21 shows plots of $\Delta\Phi(r)$ for different values of $\Delta\mu \equiv \mu_C - \mu$.
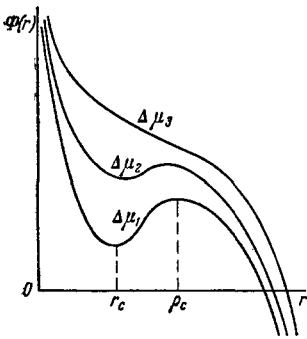

FIG. 21. Energy of formation of an etch nucleus with radius r.

When $\Delta\mu < \Delta\mu_m = \dfrac{\pi\alpha^2\Omega}{Gb^2}$, both a minimum and a maximum of $\Delta\Phi(r)$ exist. The minimum, at $r = r_C$, corresponds to the formation of a hollow cylinder of radius r_C along the entire dislocation line; the surface energy gain involved in the formation of the walls of this channel is smaller than the loss incurred when the strained region around the dislocation line is removed from the crystal (in the case of a large Burgers vector). The maximum of $\Delta\Phi(r)$ at $r = \rho_C$ determines the energy barrier for the formation of critical nuclei. With increasing $\Delta\mu$ the values of ρ_C and r_C approach each other, the barrier disappears, and etch channel is formed near the dislocation without surmounting a potential barrier.[46,118,119] When $\Delta\mu > \Delta\mu_C$ the dislocation "is exposed."

The strains around a dislocation, which lead to the considered effect, also accelerate the crystal dissolution (or evaporation) caused by a screw dislocation. The strains increase the angular velocity of rotation of the spiral step[46] (Fig. 22).

Orlov and Fishman[120] have considered phenomenologically the diffusion kinetics of the appearance of an etch pit at a dislocation, starting with the assumption that the macroscopic rate of dissolution at each sur-
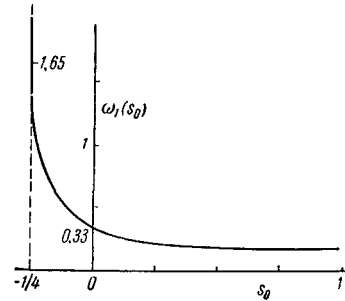

FIG. 22. Angular velocity of rotation ω of a spiral (in the unit v_0/ρ_C) as a function of the parameter $s_0 = \dfrac{Gb^2\Delta\mu}{8\pi\alpha^2\Omega}$.

face point is $\sim \mu_C - \mu$ $\left(\mu_C = \mu_{C_0} + \dfrac{Gb^2}{4\pi r^2}\right)$ and is independent of the surface orientation, i.e., of step density. In reference 120 the depth of the pit at the point of emergence of a dislocation is given as $\sim \sqrt{t}$, where t is the etching time; the role of surface energy is not considered.

It is obvious that etch pits can appear at dislocations only when the dislocations are the strongest source of steps on the surface. For example, if the density of steps coming from the crystal edge exceeds the density resulting from dislocations under the given conditions, then the normal dissolution rate will be approximately uniform over the entire surface and etch pits cannot be formed.

Amelinckx, Bontinck, and Dekeyser[122] have proposed a kinematic scheme for the formation of macroscopic spiral layers in the process of evaporation at a helicoidal dislocation. The line of a helicoidal dislocation in a crystal is twisted spirally so that its point of intersection with the surface, i.e., the center of the spiral step in the etching process, moves circularly. A macroscopic spiral results from this "wobbling" (Fig. 23). The height of the macrostep therefore equals the screw pitch of the helicoidal dislocation. Lang[123] had somewhat earlier discussed "wobbling" for the case in which the step sources are nuclei of growth or dissolution with their centers on a circle. References 122 and 123 do not consider the dependence of the rate of advance of steps on their density.

The chemical potential of a crystal near the point of emergence of a dislocation depends essentially on the segregation of impurities at dislocations.[124,125] This plays an important part in metals, where etch pits are not usually formed in the absence of impurities.[125]

VI. COLLECTIVE EFFECTS IN THE MOVEMENT OF STEPS

The discussion and experimental data presented in the preceding sections show that the stepped structure of a crystal surface depends on the conditions of growth — supersaturation, temperature, and the presence of impurities. On the other hand, growth in-
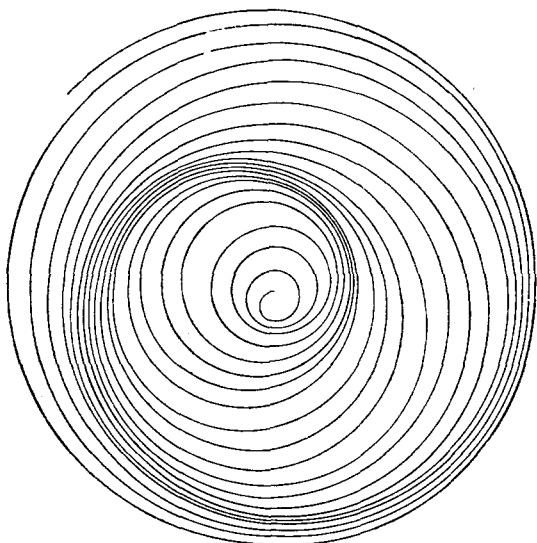
FIG. 23. The circular movement of the center of a spiral step leads to the bunching of steps; the result is a spiral with a much greater distance between turns.

volves the movement of steps, so that the surface structure affects the growth rate and the properties of the resulting crystal. Some examples of this are the dependence of the coefficient of nonuniform impurity capture on the heights and distances between steps (Sec. 20), the nonuniform influence of certain impurities on the velocities of steps of different heights (Sec. 19), the influence of the number of spiral turns on the normal growth rate (Sec. 10) etc. The surface structure is therefore, at least in some cases, a connecting link between the growth conditions and properties of a crystal.

In the present section we shall consider some processes in the formation of a stepped topography, concentrating our attention on collective effects that accompany step movement rather than on the shapes, stability and rates of advance of individual steps. We shall investigate the generation, motion and disappearance of kinematic ("shock") condensation waves of individual steps. The second section treats the kinetic equation for steps of different heights and presents some solutions of the equation. For one special case we determine the temporal dependence of the increase of mean step height due to the merging of steps.

22. "Shock Waves" of Step Density

It was shown in Ch. II and III that the rate of advance of a sequence of elementary steps depends on the distance between the steps, i.e., on the number of steps intersecting a unit line segment parallel to the x axis and perpendicular to the step fronts. This "step density," which depends in general on both x and t, will be denoted by $\rho(x,t)$. If a is the height of each step, then $a\rho$ is the tangent of the angle of inclination of the macroscopic face formed by the

steps. The rate of step advance is $v(|\rho|)$.[*]

With conservation of the number of steps, the density $\rho(x,t)$ must satisfy the equation[†]

$$\frac{\partial \varrho}{\partial t} + \frac{\partial}{\partial x}(\varrho v) = 0. \qquad (22.1)$$

The step current $J \equiv \rho v$ multiplied by the step height is the normal rate of growth (or dissolution, or melting) of the face formed by the given steps. For increased values of ρ the rate of advance decreases and $\frac{\partial^2 J}{\partial \rho^2} < 0$. $\rho(x,t)$ is constant for values of x and t lying on the characteristics of Eq. (22.1), i.e., they satisfy the equation $\frac{dx}{dt} = \frac{\partial J(\rho)}{\partial \rho}$ for the corresponding values of ρ.

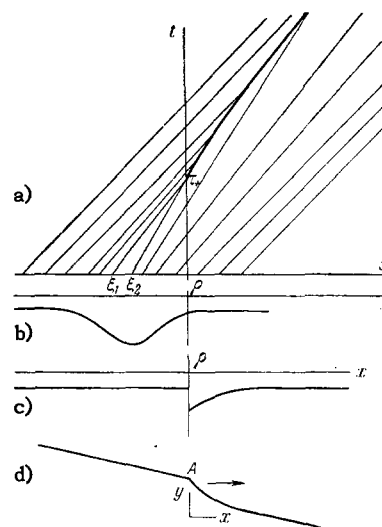At initial time, t = 0, let the step density distribution $\rho_0(x)$ have the character depicted in Fig. 24b.

FIG. 24. Formation (a) of a step density discontinuity [at x = 0 (c)] from an initial perturbation $\rho_0(x)$ (b). (d) is the surface profile.

Drawing characteristics with slopes $\left.\dfrac{\partial J}{\partial \rho}\right|_{\rho_0(x)}$ from each point of the x axis, we find that a discontinuity of step density arises at a time τ_+ (Fig. 24a), i.e., a corner A (Fig. 24d) appears in the surface profile. The velocity of advance V_t of this discontinuity of elementary step density (i.e., of the kinematic or "shock" wave of the steps) is determined from the conservation of the number of steps at the density discontinuity point, whose position on the x axis obeys a law x = X(t):

$$\varrho_1(v_1 - X_t') = \varrho_2(v_2 - X_t'),$$

---

[*] ρ can be taken as positive or negative, depending on the sine of the inclination angle of the vicinal face formed by the steps under consideration.

[†] This equation is a special case of the general kinetic equation for steps that was formulated by the authors in 1957 and that is discussed in Sec. 23.

or

$$V_t = X'_t = \frac{J_2 - J_1}{\varrho_2 - \varrho_1}, \qquad (22.2)$$

where $J_1 = J(\rho_1)$ and $J_2 = J(\rho_2)$, while ρ_1 and ρ_2 are the values of the step density on both sides of the discontinuity. [The denominator $\rho_2 - \rho_1$ thus represents the discontinuity of the tangent of the crystal surface angle at the corner A (Fig. 24d), divided by the step height.] The formation of "shock waves" of steps was first investigated by Frank,[56] and also by Cabrera and Vermilyea,[87] using the general analysis of kinematic waves by Lighthill and Whitham.[126] The formation of packets of elementary steps in growth from the melt was earlier investigated qualitatively by Elbaum and Chalmers.[73] The combining of steps was discussed still earlier by Volmer.[32,117]

We shall now study in greater detail, by analogy with the general theory in reference 126, the formation of a density discontinuity and its temporal evolution.[128] Let us consider, specifically, the case of growth where $v > 0$ and $\rho < 0$. The initial form of the density perturbation is given as a function $\rho_0(x)$ such that $\rho_0(\pm\infty) = \rho_\infty = \text{const}$ (Fig. 24b). The perturbation can result, for example, from a momentarily increased strength of the screw dislocation that served as the source of the step sequence. The increased strength can result from a random rise of supersaturation or from breakdown of the spiral step (Sec. 10). Other kinds of perturbation will be considered below.

Since the step density is constant along each characteristic $x = \xi + \left.\frac{\partial J}{\partial \rho}\right|_{\rho_0(\xi)} t$ (where ξ is the value of x at $t = 0$ and $\rho = \rho_0$), the discontinuity arises after the time τ_+ given by

$$\tau_+ = -\frac{\xi_2 - \xi_1}{J'(\varrho_0(\xi_2)) - J'(\varrho_0(\xi_1))} \sim -\frac{1}{J''(\varrho_\infty)\frac{d\varrho_0}{dx}},$$

where

$$J' = \frac{\partial J}{\partial \varrho}, \qquad J'' = \frac{\partial^2 J}{\partial \varrho^2},$$

and ξ_1 and ξ_2 are values of x depending on the shape of the initial perturbation, the difference between them being of the order of magnitude of the half-width of the perturbed region. The higher the supersaturation, the more abrupt the initial perturbation; also, the greater the anisotropy of the normal growth rate, the more rapidly will density discontinuities arise. In estimating τ_+, we let $-aJ \sim a^{-1}J'' \sim 10^{-5}$ cm/sec and $\frac{d\rho_0}{dx} \sim -10^{10}$ cm^{-2}. The latter value is obtained when $-\rho \sim 10^6$ cm^{-1} (corresponding to $\sim 2°$ face inclination), $\rho_2 - \rho_1 \sim 10^6$ cm^{-1}, and $\xi_2 - \xi_1 \sim 10^{-4}$ cm. (This value corresponds to the tangential velocity $v = J/\rho = 3 \times 10^{-4}$ cm/sec if the perturbation occurs during a time ~ 0.3 sec). Then $\tau_+ \sim 3 \times 10^2$ sec. An

improvement of the selected numerical values can only increase τ_+, in our opinion. Therefore the described formation of density discontinuities could be observed experimentally.

We shall now give the law of motion of a density discontinuity and the change of its magnitude in time. Since we are interested in the behavior of an already existing discontinuity, we can let it have the form depicted in Fig. 24c [$\rho_0(x) = \rho_\infty$ for $x < 0$] and assume $\rho_1 = \rho_\infty$ in (22.2).

We replace t with the new variable ξ, the x-coordinate of that step density at $t = 0$ which at the later time t determines the density discontinuity in the shock wave:

$$X(\xi) = \xi + J'(\varrho_0(\xi)) t. \qquad (22.3)$$

The differential equation for $X(\xi)$, obtained from (22.2) and (22.3), is solved subject to the initial condition $X(0) = 0$, giving

$$X(\xi) = \xi + \exp\left(\int \Phi(\xi) d\xi\right) \int_0^\xi F(\xi) \exp\left(-\int \Phi d\xi\right) d\xi, \qquad (22.4)$$

where

$$\Phi(\xi) = \frac{J_0 - J_\infty}{\varrho_0 - \varrho_\infty}\frac{J''\varrho_0'}{J'}\left[\frac{J_0 - J_\infty}{\varrho_0 - \varrho_\infty} - J_0'\right]^{-1}, \qquad F(\xi) = J_0'\left[\frac{J_0 - J_\infty}{\varrho_0 - \varrho_\infty} - J_0'\right]^{-1}$$

Equations (22.3) and (22.4) determine $t(\xi)$ and $X(\xi)$, representing the exact solution of the problem in parametric form. If $\rho_0(\xi) - \rho_\infty$ is small, then up to terms of the order $\rho_0(\xi) - \rho_\infty$ we have

$$X(\xi) = \xi - \frac{2J'_\infty}{J''_\infty(\varrho_0 - \varrho_\infty)^2}\int_0^\xi(\varrho_0 - \varrho_\infty) d\xi. \qquad (22.5)$$

Putting $t \to \infty$, we obtain $\rho_0 \to \rho_\infty$ and $X'_t \to J'_\infty$; the shock wave thus tends to be smoothed out into a uniform step sequence.

When t and ξ are large, the integral in (22.5) can be extended to infinity, and in conjunction with (22.3) leads to the asymptotic formula

$$\varrho_0 - \varrho_\infty \sim \frac{1}{\sqrt{t}}\left(-\frac{2}{J''_\infty}\int_0^\infty(\varrho_0 - \varrho_\infty) d\xi\right)^{1/2}, \qquad (22.6)$$

from which it follows that the magnitude of the density discontinuity decreases as $\sim t^{-1/2}$. A kinematic wave of elementary steps should appear visually as a smeared macroscopic step of total height $a\int_0^\infty(\rho(x) - \rho_\infty) dx$. It follows from (22.5) that this macrostep is smeared more and more; experimentally this can look like a reduction of step height, although the overall height actually remains constant. The time τ_- for the "disappearance" of a kinematic wave is reasonably defined as the time required to reduce the density discontinuity $\rho_0 - \rho_\infty$ to a given value depending on the conditions of observation. τ_- is inversely proportional to the supersaturation [see Eq.

(22.6)] and the path traversed by the discontinuity during this time is practically independent of super-saturation.[128]

Thus a perturbation of the density of elementary steps results in the production of a "shock wave," after which the perturbation is smoothed out. The relaxation times τ_+ and τ_-, and the path traversed by the perturbation before disappearing, are large enough to permit observation.

Density perturbations of the type shown in Fig. 24d are not the only ones possible. A density discontinuity will result from many different kinds of perturbations that produce a surface region where the absolute value of the step density is enhanced (see the equation for τ_+). Figure 25 shows some of the permissible surface profiles.
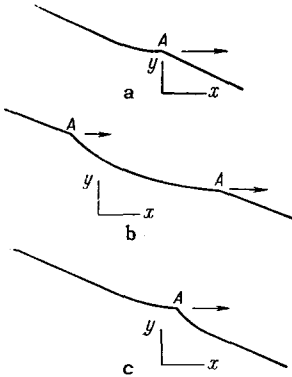
FIG. 25. Some of the conceivable surface profiles involved in the production of shock waves.

The kinematic wave contains a discontinuity of elementary step density, i.e., the surface profile exhibits a macroscopic corner, to the left and right of which the slopes vary in time and differ from those required by surface energy anisotropy (Ch. I). No inconsistency arises if the expression for J takes surface energy into account, as follows:

$$J = J(\varrho, \varrho'_x) = \varrho v(|\varrho|)\left[1 + \frac{\Omega}{a(\mu_m - \mu_{C0})}\frac{\partial^2 F}{\partial \varrho^2}\frac{\partial \varrho}{\partial x}\right],$$

where μ_m and μ_{C_0} are the chemical potentials of the medium and crystal, respectively. At low elementary step density ρ there is practically no energetic interaction between steps, $\frac{\partial^2 F}{\partial \rho^2}$ is small, and surface energy plays no important part (Sec. 5). Therefore for sufficiently small departures of the crystal surface from close-packed orientation, energy effects can be neglected while kinematic phenomena alone are considered, as in the present section. All results obtained here can obviously be extended to the cases of crystal dissolution, evaporation etc.

Macroscopic steps of two types can therefore exist on crystal surfaces. First, for the "true" steps, stability is determined by surface energy anisotropy; these steps have a stationary shape and constant rate of advance. The second type comprises macrosteps which are weak kinematic waves of elementary step density. Kinematic waves with large densities should become steps of the first type; this can be one of the mechanisms responsible for the formation of "true" steps.

It is difficult to determine which type of steps exists on any real surface, in the absence of direct investigations of step profiles. The available observations of growth steps[129] point to their relative stability (at low supersaturations) and constant rate of advance, which diminishes with height approximately as 1/h and is independent of the separation of successive steps until their almost complete merger. These are evidently steps of the first type. However, the fronts of growth steps have been observed to depart as little as $1:200$ from a close-packed face.[130] Sometimes the gradual disappearance of macrosteps is observed, accompanied by an accelerated rate of advance;[49] these steps can be treated as kinematic waves. Some dissolution macrosteps also resemble kinematic waves.[66]

23. A Kinetic Equation for Steps

We have so far considered only the collective motion of steps with <u>identical</u> heights, whereas a real crystal surface includes many macro- and microsteps with different heights and different rates of advance that make merging possible. The breakdown of steps is also possible. A statistical description of the stepped structure of a surface is required by the very large number of steps.

We shall first consider the case of "true" steps, assuming a constant rate of advance for each step up to the instant of merger with another step. We introduce the step distribution function (or density) $\rho(m, r, t)$, where r is the radius vector of a point on the surface and m is step height expressed in interatomic spacings. ρ is the number of steps intersecting a unit line segment perpendicular to the step fronts and passing through the point r. The relative rate of advance of two steps with heights m and m' is $v(m) - v(m') \equiv |\sigma| f(m, m')$. Finally, $w(\mu, \nu)$ will denote the probability per unit time that a step with height ν will be detached from a step with height μ. The following kinetic equation is obeyed by ρ:

$$\frac{\partial \varrho}{\partial \tau} + \operatorname{div} \varrho v n = \int_0^{\frac{m}{2}} \varrho(\nu, r, t) f(\nu, m-\nu)\varrho(m-\nu, r, t)d\nu$$

$$- \varrho(m, r, t)\left[\int_0^m \varrho(\nu, r, t)f(\nu, m)d\nu\right.$$

$$\left. + \int_m^\infty \varrho(\nu, r, t)f(m, \nu)\right]d\nu + \int_m^{2m}\varrho(\nu, r, t)w(\nu, \nu-m)d\nu$$

$$+ \int_{2m}^\infty \varrho(\nu, r, t)w(\nu, m)d\nu - \varrho(m, r, t)\int_0^{\frac{m}{2}} w(m, \nu)d\nu,$$

(23.1)

where $\tau = |\sigma|t$, the vector n is normal to the step

front and lies in the plane of the close-packed face
(Fig. 7), and $v = v(n)$. Equation (23.1) describes
processes in both growth and dissolution, as distin-
guished by the sign of the supersaturation. We shall
discuss some deductions from this equation.

1. Kinematic waves. If all steps are identical in
height $[\rho \sim \delta(m - m_0)]$ and cannot break down, then
steps do not merge; the right-hand side of (23.1) thus
disappears leaving the simple equation (22.1) already
considered in Sec. 22, with the stationary solution
ρ = const and the nonstationary solution representing
a kinematic density wave. If at initial time $\rho \sim \delta$
$\times (m - m_0)$, but $w \neq 0$, the right-hand side does not
vanish, and in time ρ as a function of m is "smeared,"
i.e., steps both higher and lower than m_0 appear.

2. The equation of a spiral. If $\rho(m, r, t)$
$= \delta(m - m_0)\delta(r - r(\theta, t))$ and $w = 0$, the right-hand
side of (23.1) disappears, while the left-hand side,
after multiplication by n, gives the equation of motion
of a step:

$$\left(n \frac{\partial r}{\partial t}\right) - v = 0. \qquad (23.2)$$

In the steady case where $r(\theta, t) = r_0(\theta) + \omega \times r_0 t$,
Eq. (23.2) has the spiral solution described in Sec. 9
$[\omega \perp r, n$ (Fig. 7)].

3. Growth and dissolution shapes. Equation (23.2)
also permits a step contour $r = r_0(\theta)$ that remains
similar with the lapse of time. If $r(\theta, t) = r_0(\theta)\frac{t}{t_0}$,
we obtain

$$(nr_0) = v(n) t_0, \qquad (23.3)$$

where t_0 is a constant. Replacing $v(n) t_0$ with $\alpha(n)\Lambda^{-1}$
gives Eq. (2.3) for a family of straight lines whose en-
velope represents the equilibrium shape of the crystal
(Sec. 2). Therefore a stationary growth shape, the en-
velope of the family (23.3), is plotted on the polar dia-
gram of $v(n)$ according to the Wulff theorem. This
rule for constructing growth and dissolution shapes of
crystals was proposed in geometric form by Gross[132]
as early as 1918; see also reference 133. These early
investigators also studied the geometry of etch pits.
By analogy with (2.2) and (2.3), Eq. (23.3) can be con-
sidered the solution of the variational problem
$\int v(n) ds$ = min. A condition for the stable (similarity)
transformation (23.3) in growth is $v + v''_{\theta\theta} > 0$, and in
dissolution, $v + v''_{\theta\theta} < 0$. The "inner" envelope of the
family (23.3) must correspond to the stationary growth
shape, while the outer envelope (Fig. 26) corresponds
to the stationary dissolution shape. $v + v''_{\theta\theta}$ = const
must hold true over the entire surface of the station-
ary shape. Taking r_0 and n to be three-dimensional
vectors, Eq. (23.3) can be used to derive the growth
shape of a three-dimensional crystal, not merely of a
step. According to the kinematic theory of nonstation-
ary shapes developed by Frank[56] the shape changes in
such a way that surface regions with given orienta-
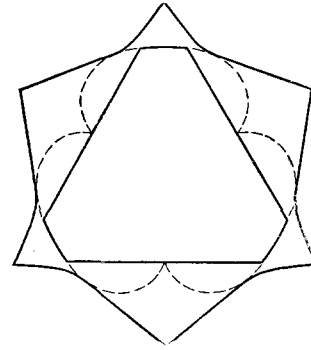

FIG. 26. The dashed curve is the polar diagram of growth rates.
The closed solid lines are Wulff envelopes of v(n). The inner line
gives the stationary shape for growth; the outer line gives that for
dissolution.

tions move along straight paths in the directions of
normals to the polar diagram of reciprocal velocities
$v^{-1}(n)$.

The velocity $v(n)$, like $\alpha(n)$ has sharp minima
for orientations of n corresponding to close-packed
faces. These faces can therefore be present on both
equilibrium shapes and growth shapes, although the
given correspondence is not required for all faces,
not to mention their sizes. Both growth and equilib-
rium shapes depend essentially on the structure, but
are not related directly, since the former are deter-
mined kinetically, and the latter are determined
thermodynamically.

It has been assumed above that the normal growth
rate depends only on face orientation, although the rate
is actually determined, in addition, by the macroscopic
diffusion and thermal fields around the crystal. As a
result the equilibrium shapes for both growth and dis-
solution can be modified and unstable shapes (den-
drites, cellular structure etc.) can appear.

4. The development of stepped roughness.[131] We
shall now consider the case where, at the initial time,
steps of different heights, which are unable to break
down, are distributed uniformly on the surface
$[\rho = \rho(m, \tau)]$. The lower steps, having greater ve-
locities, overtake and merge with higher steps to
form still higher steps. The mean step height varies
with time as follows:

$$\overline{m}(\tau) = \frac{\int_0^\infty m\varrho(m, \tau) dm}{\int_0^\infty \varrho(m, \tau) dm}. \qquad (23.4)$$

It follows clearly and directly from (23.4) that

$$\int_0^\infty m\varrho(m, \tau) dm = \int_0^\infty m\varrho(m, 0) dm = \frac{\overline{p}}{a} = \text{const}, \qquad (23.5)$$

where $\overline{p}$ is the tangent of the mean angle of inclination
of the stepped surface. $\int_0^\infty \rho dm$ is easily determined
for the case in which $f(m, m')$ is a homogeneous

function of the degree $-k$, i.e., $f(\lambda m, \lambda m') = \lambda^{-k} \times f(m, m')$, and the solution of (23.4) can be put into the form

$$p(m, \tau) = (\tau + \tau_0)^{-s} \varphi(m(\tau + \tau_0)^{-q}),$$

where τ_0, s and q are constants. The values of these constants must be such that $\int_0^\infty m\rho \, dm$ is not time-dependent and (23.4) is satisfied by a function φ of a single variable. This is possible when

$$s = 2q, \quad q = \frac{1}{(k+1)}.$$

Hence the temporal increase of mean step height is given by

$$\overline{m} = C\overline{p}(\tau + \tau_0)^{\frac{1}{k+1}}, \quad C^{-1} \int_0^\infty \varphi(\xi) \, d\xi. \tag{23.6}$$

When $k = 1$ we have $\overline{m} \sim \overline{p}\sqrt{\sigma t}$, and the mean step density decreases as $(\sigma t)^{-1/2}$.

The foregoing description of the establishment of macroscopic surface roughness has limited application. Martynov and Bakanov[134] have shown* that the asymptotic behavior of the equation for the coagulation of sols, which is similar to (23.4) and was investigated earlier by Todes,[135] depends on the <u>initial</u> distribution, so that φ is not a universal function for all distributions. Equation (23.6) is thus rigorously accurate only if the initial distribution is given by φ. This equation therefore furnishes only a qualitative estimate of the coagulation process.

When the coalescence of steps is compensated by breakdown, a steady-state step-height distribution is established, described by a function $w(\mu, \nu)$. The height distribution of low steps is given by $\rho(m)$ = $w(m) \, v(m)$, if $w(\mu, \nu) = w(\mu)$, i.e., the frequency with which steps of a given height are emitted does not depend on the height μ of the disintegrating step. This relationship expresses the kinematic stability of a macrostep, which results when the current ρv of low steps that merge with it equals the current w of emitted steps.

A complete stationary distribution function $\rho(m)$ and general asymptotic laws for the nonstationary processes of step coalescence have not yet been found.

Howes[136] recently undertook an experimental investigation of the temporal change of stepped surface roughness in line with the foregoing discussion. He studied the electrodeposition of copper on a surface forming a small angle with (100), obtaining the step-height distribution at successive 15-minute intervals (Fig. 27). Unfortunately, the experimental technique was limited to macrosteps above ~ 0.1 micron. Figure 27 shows clearly the reduced density of low steps that merge with high steps, the appearance of a dis-

*The author is indebted to G. A. Martynov and S. P. Bakanov for communicating their results before publication.

tribution peak, and the shift of this peak toward higher steps. The mean distance $\overline{\lambda}$ between steps increases with time according to $\overline{\lambda} = c_1\sqrt{t} + c_2$, and c_1 and c_2 are constants (Fig. 28). The data in reference 136 thus agree qualitatively with the statistical theory. It would be highly desirable to have further experiments taking lower steps into account (down to elementary steps), for different mean orientations of the stepped surface; also, experiments to determine the disintegration function w, and to investigate the effects of impurities and of supersaturation on stationary and nonstationary distributions ρ both in crystal growth from different media and in decrystallization.
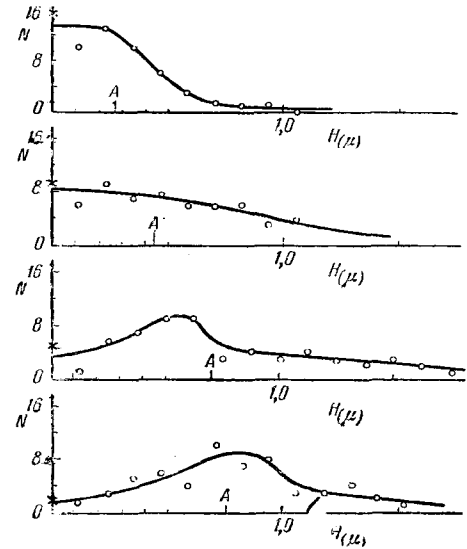

FIG. 27. The distribution of step heights H at 15-minute intervals.
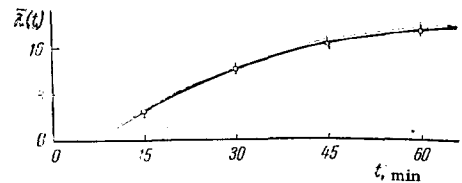

FIG. 28. Mean step separation as a function of time.

[1] J. W. Gibbs, Thermodynamical Works III. On the Equilibrium of Heterogeneous Substances, Gostekhizdat, Moscow, 1950, pp. 328, 409.

[2] M. Volmer, Kinetik der Phasenbildung, Steinkopf Verlag, Dresden and Leipzig, 1939.

[3] W. Kossel, Nachr. Ges. Wiss. Göttingen, Math.-Physik. Kl., 153 (1957).

[4] I. N. Stranski, Z. physik. Chem. 136, 259 (1928).

[5] I. N. Stranski, Z. physik. Chem. B11, 342 (1931).

[6] I. N. Stranski and R. Kaischew, Z. Krist. 78, 373 (1931).

[7] I. N. Stranski and R. Kaischew, Z. physik. Chem. B26, 317 (1934).

[8] I. N. Stranski and R. Kaischew, Physik. Z. 36, 393 (1935).

[9] I. N. Stranski and R. Kaischew, Usp. Fiz. Nauk 21, 408 (1939).

[10] R. Becker and W. Döring, Ann. Physik 24, 719 (1935).

[11] J. Sears, J. Chem. Phys. 24, 868 (1956).

[12] F. C. Frank, Discussions Faraday Soc. 5, 48 (1949).

[13] Ya. I. Frenkel', JETP 16, 39 (1946).

[14] Burton, Cabrera, and Frank, Phil. Trans. Roy. Soc. (London) A243, 299 (1951), Russ. transl. in ref. 143.

[15] P. Ehrenfest, Ann. Physik 48, 360 (1915).

[16] M. Yamada, Physik. Z. 24, 364 (1923); 25, 52, 289 (1924).

[17] L. D. Landau, Symposium in Commemoration of the 70th Birthday of A. F. Ioffe, Acad. Sci. Press, Moscow, 1950, p. 44.

[18] C. Herring, Surface Tension as a Motivation for Sintering, in Collection, Physics of Powder Metallurgy, McGraw-Hill, New York, 1951, p. 143.

[19] C. Herring, The Use of Classical Macroscopic Concepts in Surface Tension Problems, in Collection, Structure and Properties of Solid Surfaces, New York, p. 5.

[20] A. A. Chernov, Кристаллография 3, 227 (1958), Soviet Phys.-Crystallography 3, 225 (1959).

[21] L. D. Landau and E. M. Lifshitz, Статистическая физика, (Statistical Physics), Gostekhizdat, Moscow, 1951, p. 455.

[22] I. M. Lifshitz and A. A. Chernov, Кристаллография 4, 788 (1959), Soviet Phys.-Crystallography 4, 747 (1960).

[23] A. A. Chernov and E. D. Dukova, Кристаллография 5, 655 (1960), Soviet Phys.-Crystallography 5, 627 (1961).

[24] V. D. Kuznetsov, Поверхностная энергия твердых тел. (The Surface Energy of Solids), Gostekhizdat, Moscow, 1954.

[25] G. G. Lemmlein, Doklady Akad. Nauk S.S.S.R. 78, 685 (1951).

[26] M. O. Kliya, Dissertation, Institute of Crystallography, Acad. Sci. U.S.S.R., 1952.

[27] M. O. Kliya, Кристаллография (Crystallography) 1, 576 (1956).

[28] P. I. Lukirskii, Doklady Akad. Nauk S.S.S.R. 46, 274 (1945).

[29] Ya. E. Geguzin and N. N. Ovcharenko, Doklady Akad. Nauk S.S.S.R. 99, 389 (1954); Izv. Akad. Nauk S.S.S.R., Ser. Tekh. No. 1, 108 (1956).

[30] A. J. W. Moor, Acta Met. 6, 293 (1958).

[31] D. A. Young and A. T. Gwatemy, J. Appl. Phys. 31, 225 (1960).

[32] M. Volmer, Z. physik. Chem. 102, 267 (1922).

[33] C. M. Heck, Phys. Rev. 51, 686 (1937).

[34] Communication concerning the report of G. G. Lemmlein at a session of the Division of Physical and Mathematical Sciences of the U.S.S.R. Academy of Sciences, Vestnik Akad. Nauk S.S.S.R. No. 4, 119 (1945).

[35] G. S. Zhdanov, Doklady Akad. Nauk S.S.S.R. 48, 39 (1945); G. S. Zhdanov and Z. V. Minervina, Doklady Akad. Nauk S.S.S.R. 48, 182 (1945); JETP 15, 655 (1945), 17, 3 (1947).

[36] M. Brandstetter, Z. Elektrochem. 56, 168 (1952); 57, 438 (1953).

[37] S. Amelinckx and W. Dekeyser, Les dislocations et la croissance des cristaux, Paris, 1956.

[38] S. Amelinckx, Naturwissenschaften 39, 547 (1952).

[39] A. J. Forty, Direct Observations of Dislocations in Crystals, Advances in Physics 3, 1 (1954).

[40] G. W. Sears, J. Chem. Phys. 23, 1630 (1955).

[41] K. M. Gorbunova, Report at the First Conference on Crystal Growth, Moscow, 1956, "Рост кристаллов" (Growth of Crystals), vol. I, Acad. Sci. Press, Moscow, 1957, p. 48.

[42] T. V. Ivanovskaya, On Some Laws of Electrolytic Crystal Growth which Determine the Lustre of Metallic Coatings, Dissertation, Moscow, 1955.

[43] Kaischew, Budewski, and Malinowski, Z. physik. Chem. 204, 348 (1955).

[44] A. R. Verma, Crystal Growth and Dislocations, Academic Press, New York, 1954.

[45] R. S. Mitchell, Phil. Mag 46, 1141 (1955).

[46] N. Cabrera and M. M. Levine, Phil. Mag. 1, 450 (1956).

[47] N. Cabrera, J. Chem. Phys. 21, 1111 (1953), Russ. transl. in reference 143.

[48] M. Volmer and W. Schultze, Z. physik. Chem. A156, 1 (1931).

[49] G. G. Lemmlein and E. D. Duskova, Spiral Growth of p-toluidine Crystals, Motion picture film, Institute of Crystallography, Acad. Sci. U.S.S.R., 1956.

[50] C. W. Bunn and H. Emmett, Discussions Faraday Soc. 5, 119 (1949).

[51] G. G. Lemmlein and E. D. Dukova, Кристаллография (Crystallography) 1, 112 (1956).

[52] M. I. Kozlovskii and G. G. Lemmlein, Кристаллография 3, 351 (1958), Soviet Phys.-Crystallography 3, 352 (1959).

[53] A. A. Chernov, Кристаллография (Crystallography) 1, 119 (1956).

[54] J. P. Hirth and G. M. Pound, J. Chem. Phys. 26, 1216 (1957).

[55] G. W. Sears, J. Chem. Phys. 27, 1308 (1957).

[56] F. C. Frank, op. cit. ref. 142, p. 411.

[57] A. A. Noyes and W. R. Whitney, Z. physik. Chem. 23, 689 (1897).

[58] W. Nernst, Z. physik. Chem. 47, 52 (1904).

[59] A. Berthoud, J. de chim. phys. 10, 624 (1912).

[60] A. Bravais, Étude cristallographique, Paris, 1866.

[61] P. Niggli, Z. anorg. Chem. 110, 55 (1920).

[62] W. B. Hillig and D. Turnbull, J. Chem. Phys. 24, 914 (1956), Russ. transl. in ref. 143.

[63] A. A. Chernov, Doklady Akad. Nauk S.S.S.R. **133**, 1323 (1960).

[64] R. Marc, Z. physik. Chem. **61**, 385 (1908).

[65] W. Wenk, Z. Krist **47**, 124 (1910).

[66] M. I. Kozlovskii, An Experimental Investigation of Crystal Growth in the Light of the Dislocation Theory, Dissertation, Moscow State University, 1958.

[67] W. J. Dunning and N. Albon, op. cit. ref. 142, p. 446.

[68] M. Follenius, Bull. soc. franc. min. crist. **82**, 343 (1959).

[69] K. A. Jackson, op. cit. ref. 142, p. 319.

[70] B. Chalmers, op. cit. ref. 142, p. 291.

[71] V. I. Malkin, The Mechanism of Crystal Growth and the Formation of Structure in Crystallization from the Melt, Dissertation, Central Research Institute of Ferrous Metallurgy, 1952.

[72] L. Graf, Z. Metall. **42**, 336 (1951).

[73] C. Elbaum and B. Chalmers, Can. J. Phys. **33**, 196 (1955).

[74] W. A. Tiller, J. Metals **9**, 847 (1957).

[75] W. A. Tiller, J. Appl. Phys. **29**, 611 (1958).

[76] D. Turnbull, Phase Changes, Solid State Physics 3, 225 (1956).

[77] W. Hillig, op. cit. ref. 142, p. 350.

[78] Lindenmeyer and B. Chalmers, op. cit. ref. 142, p. 308.

[79] M. Volmer and M. Marder, Z. physik. Chem. **A154**, 97 (1931).

[80] H. Pollatschek, Z. physik. Chem. **142**, 289 (1929).

[81] A. Rosenberg and W. C. Winegrad, Acta Met. **2**, 342 (1954).

[82] D. Gernez, Compt. rend. **95**, 1278 (1882).

[83] Powell, Gilman, and Hildebrand, J. Am. Chem. Soc. **73**, 2525 (1951).

[84] A. Seeger, Phil. Mag. **44**, 1 (1953).

[85] G. G. Lemmleïn, Секториальное строение кристаллов, (The Sector Structure of Crystals), Acad. Sci. Press, Moscow, 1948.

[86] H. E. Buckley, Crystal Growth, Wiley, New York, 1951.

[87] N. Cabrera and D. A. Vermilyea, loc. cit. ref. 142, p. 393.

[88] Gilman, Johnston, and Sears, J. Appl. Phys. **29**, 747 (1958), Russ. transl. in reference 143.

[89] G. Bliznakow and E. Kirkowa, Z. physik. Chem. **206**, 271 (1947).

[90] H. Fischer, Elektrolytische Abscheidung und Elektrokristallization von Metallen, Springer Verlag, Berlin, 1954.

[91] J. E. B. Randles and K. W. Somerton, Trans. Faraday Soc. **48**, 951 (1952).

[92] I. N. Stranski, Z. Elektrochem. **35**, 393 (1929).

[93] R. Lackman and I. N. Stranski, op. cit. ref. 142, p. 427.

[94] G. W. Sears, loc. cit. ref. 142, p. 41; J. Chem. Phys. **29**, 1045 (1958).

[95] I. N. Stranski, Bull. soc. franc. min. crist. **79**, 360 (1956).

[96] G. Bliznakow, Fortsch. Min. **36**, 149 (1958).

[97] A. A. Chernov, op. cit. ref. 41, vol. III, in press.

[98] B. Ya. Lyubov, Doklady Akad. Nauk S.S.S.R. **68**, 847 (1949).

[99] B. Ya. Lyubov, Collection, op. cit. ref. 41, vol. III, in press; Borisov, Lyubov, and Temkin, Doklady Akad. Nauk S.S.S.R. **104**, 223 (1955); D. E. Temkin, Труды ЦНИИЧМ (Trans. Central Research Institute of Ferrous Metallurgy) No. 4, 63 (1960).

[100] G. P. Ivantsov, Doklady Akad. Nauk S.S.S.R. **81**, 179 (1951).

[101] G. P. Ivantsov, op. cit. ref. 41, vol. I, p. 98.

[102] W. A. Tiller and K. A. Jackson, Acta Met. 1, 4, 428 (1953).

[103] Smith, Tiller, and Rutter, Can. J. Phys. **33**, 723 (1955).

[104] C. Wagner, J. Metals **6**, 154 (1954).

[105] A. A. Chernov, Doklady Akad. Nauk S.S.S.R. **132**, 818 (1960); op. cit. ref. 41, vol. III, in press.

[106] R. N. Hall, J. Phys. Chem. **57**, 836 (1953).

[107] M. I. Kozlovskii, Кристаллография **3**, 209 and 236 (1958), Soviet Phys.- Crystallography 3, 206 and 236 (1959).

[108] G. G. Lemmleïn and E. D. Dukova, Кристаллография (Crystallography) 1, 351 (1956).

[109] Korndorfer, Rahbek, and Sultan, Phil. Mag. **43**, 1301 (1952).

[110] A. P. Williams, Phil. Mag. **2**, 635 (1957).

[111] F. C. Frank, Verformung und Fliess des Festkörpers (Deformation and Flow of Solids), IVTAM Colloq. Madrid, 1955, Springer Verlag, Berlin, 1956, p. 73.

[112] E. Billig, Proc. Roy. Soc. (London) **A235**, 37 (1956).

[113] V. L. Indenbom, Кристаллография **2**, 594 (1957), Soviet Phys.-Crystallography 2, 587 (1959).

[114] Fischer, Fullman, and Sears, Acta Met. **2**, 344 (1954).

[115] A. J. Forty and T. G. Gibson, Acta Met. **6**, 137 (1958).

[116] R. S. Wagner, J. Appl. Phys. **29**, 1679 (1958).

[117] Regel', Urusovskaya, and Kolomiïchuk, Кристаллография **4**, 937 (1959), Soviet Phys.-Crystallography 4, 895 (1960).

[118] Cabrera, Levine, and Plaskett, Phys. Rev. **96**, 1153 (1954).

[119] N. Cabrera, J. chim. phys. et phys. chim. biol. **53**, 675 (1956), Russ. transl. in ref. 143.

[120] A. N. Orlov and S. N. Fishman, J. Phys. Chem. (U.S.S.R.), in press.

[121] I. P. Hirth and G. M. Pound, Acta Met. **5**, 649 (1957).

[122] Amelinckx, Bontinck, and Dekeyser, Phil. Mag. **2**, 1264 (1957), Russ. transl. in ref. 143.

[123] A. R. Lang, J. Appl. Phys. **28**, 497 (1957), Russ. transl. in ref. 143.

[124] N. Cabrera, in Collection, Semiconductor Surface Physics, R. H. Kingston (ed.), U. of Penn. Press, Philadelphia, 1957.

[125] D. A. Vermilyea, Acta Met. **6**, 1413 (1958).

[126] M. J. Lighthill and G. B. Whitham, Proc. Roy. Soc. (London) **A229**, 281, 317 (1953).

[127] M. Volmer and T. Erdey-Gruz, Z. physik. Chem. **A157**, 165 (1932).

[128] A. A. Chernov, Кристаллография **5**, 446 (1960), Soviet Phys.-Crystallography **5**, 423 (1960).

[129] Lemmleïn, Dukova, and Chernov, Кристаллография **2**, 428 (1957), Soviet Phys.-Crystallography **2**, 426 (1959).

[130] N. V. Gliki and V. A. Timofeeva, Кристаллография **4**, 908 (1959), Soviet Phys.-Crystallography **4**, 861 (1960).

[131] A. A. Chernov, Doklady Akad. Nauk S.S.S.R. **117**, 983 (1957).

[132] R. Gross, Nachr. Akad. Wiss. Göttingen, Math.-physik. Kl. **35**, 137 (1918).

[133] G. Fiedel, Leçons de Cristallographie, Berger-Levrault, Paris, 1926.

[134] G. A. Martynov and S. P. Bakanov, in Collection, Исследования в области поверхностных сил. (Investigations of Surface Forces), Trans. of a Conference on Surface Phenomena, ed. B. V. Deryagin (ed.), Acad. Sci. Press, Moscow, 1960.

[135] O. M. Todes, Проблемы кинетики и катализа (Problems of Kinetics and Catalysis) **7**, 137 (1949).

[136] V. R. Howes, Proc. Phys. Soc. (London) **74**, 616 (1959).

[137] A. V. Shubnikov, Как растут кристаллы, (How Crystals Grow), Acad. Sci. Press, Moscow, 1935.

[138] A. V. Shubnikov, Образование кристаллов, (The Formation of Crystals), Acad. Sci. Press, Moscow, 1947.

[139] Shubnikov, Flint, and Bokii, Основы кристаллографии, (Elements of Crystallography), Acad. Sci. Press, Moscow-Leningrad, 1940.

[140] I. V. Obreimov, The Physics of Crystals, Great Sov. Encycl., 2nd ed., v. 45, p. 16.

[141] Новые исследования по кристаллографии и кристаллохимии. (New Investigations in Crystallography and Crystal Chemistry), G. B. Bokii (ed.), Collections 1 − 2, Crystal Growth, 1950.

[142] Growth and Perfection of Crystals (Reports of International Conference on Crystal Growth) Wiley, New York, 1958.

[143] Элементарные процессы роста кристаллов (The Elementary Processes of Crystal Growth), G. G. Lemmleïn and A. A. Chernov (eds.), IIL, Moscow, 1959.

[144] J. Friedel, Les Dislocations, Gauthier-Villars, Paris, 1956.

Translated by I. Emin